https://doi.org/10.5194/tc-2020-224
Preprint. Discussion started: 21 September 2020

The Cryosphere Discussions
Open Access
EGU

Driving Forces of Circum-Antarctic Glacier and Ice Shelf Front Retreat over the Last Two Decades

Celia A. Baumhoer[1], Andreas. J. Dietz[1], Christof Kneisel[2], Heiko Paeth[2] and Claudia Kuenzer[1,2]

[1]German Remote Sensing Data Center (DFD), German Aerospace Center (DLR), Muenchner Strasse 20, D-82234 Wessling, Germany
[2]Institute of Geography and Geology, University Wuerzburg, Am Hubland, D-97074 Wuerzburg, Germany

Correspondence to: Celia A. Baumhoer (celia.baumhoer@dlr.de)

Abstract. The safety band of Antarctica consisting of floating glacier tongues and ice shelves buttresses ice discharge of the Antarctic Ice Sheet. Recent disintegration events of ice shelves and glacier retreat indicate a weakening of this important safety band. Predicting calving front retreat is a real challenge due to complex ice dynamics in a data-scarce environment being unique for each ice shelf and glacier. We explore to what extent easy to access remote sensing and modelling data can help to define environmental conditions leading to calving front retreat. For the first time, we present a circum-Antarctic record of glacier and ice shelf front retreat over the last two decades in combination with environmental variables such as air temperature, sea ice days, snowmelt, sea surface temperature and wind direction. We find that the Antarctic ice sheet area shrank 29,618±29 km^2 in extent between 1997-2008 and gained an area of 7,108±144.4 km^2 between 2009 and 2018. Retreat concentrated along the Antarctic Peninsula and West Antarctica including the biggest ice shelves Ross and Ronne. Glacier and ice shelf retreat comes along with one or several changes in environmental variables. Decreasing sea ice days, intense snow melt, weakening easterlies and relative changes in sea surface temperature were identified as enabling factors for retreat. In contrast, relative increases in air temperature did not correlate with calving front retreat. To better understand drivers of glacier and ice shelf retreat it is of high importance to analyse the magnitude of basal melt through the intrusion of warm Circumpolar Deep Water (CDW) driven by strengthening westerlies and to further assess surface hydrology processes such as meltwater ponding, runoff and lake drainage.

1 Introduction

A safety band of floating ice shelves and glacier tongues fringes the Antarctic ice sheet (Fürst et al., 2016). Large glaciers and ice shelves create buttressing effects decreasing ice flow velocities and ice discharge (De Rydt et al., 2015; Gagliardini et al., 2010; Royston and Gudmundsson, 2016). The recent large-scale retreat of ice shelfs and glacier fronts along the Antarctic Peninsula (AP) and the West Antarctic Ice Sheet (WAIS) indicates a weakening of this safety band (Cook and Vaughan, 2010; Friedl et al., 2018; Rankl et al., 2017; Rott et al., 2011). The glacier or ice shelf front is defined as the border between the ice sheet and the ocean whereby ice shelves and glaciers are the floating extensions of the ice sheet (Nicholls et al., 2009). Calving front retreat (including both, glacier and ice shelf front retreat) increases ice discharge and the

https://doi.org/10.5194/tc-2020-224
Preprint. Discussion started: 21 September 2020

contribution to global sea level rise. The current contribution of the Antarctic ice sheet to global sea level rise is 7.6± 3.9 mm (1992-2017) but over the last decades a strong trend of mass loss acceleration was observed for the WAIS after ice shelves and glaciers retreated and thinned (IMBIE, 2018). In contrast, there is no clear trend in the mass balance of the East Antarctic Ice Sheet (EAIS) as since the 1990s Altimetry measurements show very small gain (but with high uncertainties) for the EAIS with 5±46 Gt/yr (1992-2017) (IMBIE, 2018). However, calculated with the mass budget method a strong mass loss trend exists with -47±13 Gt/yr (1989-2017) (Rignot et al., 2019). Glacier terminus positions along the EAIS experienced a phase of retreat between 1974 and 1990 followed by a phase of advance until 2012. The single exception at East Antarctica is Wilkes Land with retreating glacier fronts (Miles et al., 2016).

Glacier and ice shelves are in direct interaction with atmosphere and ocean and hence sensitive to changes in environmental conditions (Domack et al., 2005; Kim et al., 2001; Vaughan and Doake, 1996; Wouters et al., 2015). Nevertheless, changes in glacier and ice shelf extent can be independent from environmental forcing as glaciers experience a natural cycle of decay and growth (De Rydt et al., 2019; Hogg and Gudmundsson, 2017). Therefore, the identification of driving forces for fluctuations in ice shelf and glacier extent is challenging and has been subject of many discussions in the past. Glacier retreat along the Antarctic Peninsula was first only associated to atmospheric warming (Cook et al., 2016; Mercer, 1978), until more recent studies identified ocean forcing as the main driver (Cook et al., 2016; Wouters et al., 2015). Additionally, the formation of melt ponds on the ice shelf surface has been discussed as an enhancing factor for calving. Meltwater can initiate crevasse propagation resulting in hydrofracture and ice shelf retreat (Scambos et al 2000, Scambos 2017). The poleward shift of the west wind drift causes upwelling Circumpolar Deep Water (CDW). This increases ocean temperatures at the bottom of ice shelves inducing basal melt and ice shelf thinning which was observed in the Bellingshausen and Amundsen Sea (Dutrieux et al., 2014; Thoma et al., 2008; Wouters et al., 2015). Especially in combination with a retrograde bed (Hughes, 1981; Scheuchl et al., 2016), the basal melt causes a retreat of the grounding line followed by increased ice discharge (Konrad et al., 2018; Rignot et al., 2013). In contrast, the retreat of calving fronts along Wilkes Land (EAIS) was associated with a reduction of sea ice days (Miles et al., 2016). The drivers of ice shelf and glacier retreat and advance can be manifold depending on studied variables, time periods and regions. So far, there has not been a comprehensive analysis comparing circum-Antarctic glacier terminus change on a continental scale within uniform time scales (Baumhoer et al., 2018). In this paper, we explore Antarctic calving front change over the last two decades by analysing Antarctic coastal change (see Figure 1) and assess the connection to changing boundary conditions. We compare changes in Antarctic calving fronts in two decadal time steps (1997-2008 and 2009-2018) to minimize the effect of short-term glacier front fluctuations. To identify potential links between calving front retreat and recent changes in the Antarctic environmental conditions, we correlated two decades of glacier change with climate data including air and sea surface temperature as well as changes in wind direction, snowmelt and sea ice cover.

https://doi.org/10.5194/tc-2020-224
Preprint. Discussion started: 21 September 2020

The Cryosphere
Discussions
Open Access

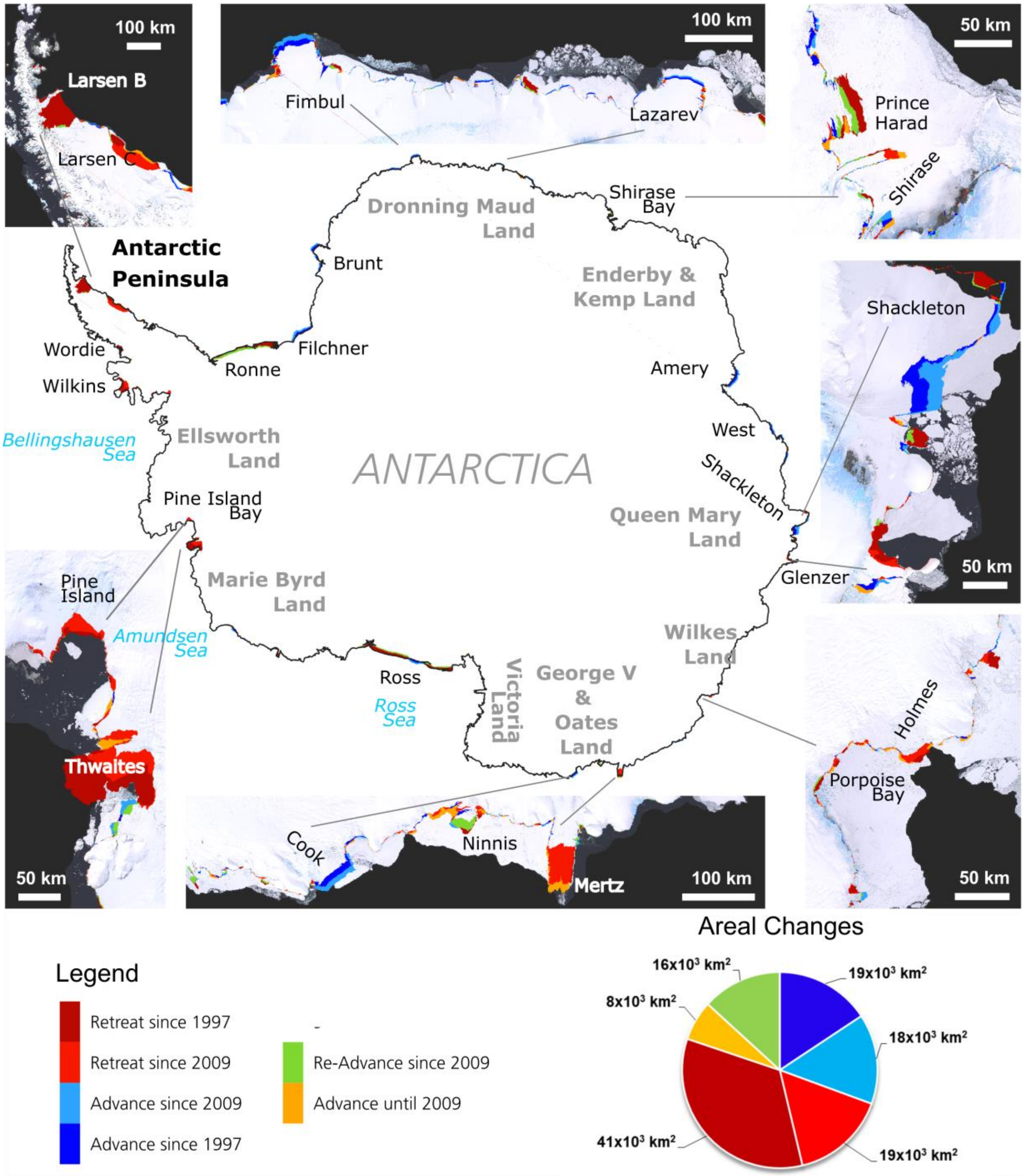

Figure 1 Coastal change of Antarctica between 1997 and 2018 with enlarged views (counter-clockwise) for Larsen C Ice Shelf, Pine Island Bay, Oates Land, Wilkes Land, Shackleton Ice Shelf, Shirase Bay and Dronning Maud Land. Colours indicate the timing of retreat and advance. The pie chart visualizes losses and gains in the area of the Antarctic ice sheet with regard to the indicated year. Background: LIMA Landsat Mosaic.

https://doi.org/10.5194/tc-2020-224
Preprint. Discussion started: 21 September 2020

2 Processed and Analysed Data Sets

2.1 Coastlines

To calculate the decadal retreat and advance of Antarctic glaciers and ice shelves, we use calving front positions of three Antarctic coastline products from 1997, 2009 and 2018. The Antarctic coastline is the border between the Antarctic ice sheet and the ocean and hence includes ice shelf and glacier front positions (Baumhoer et al., 2018). Coastal change not only includes changes in floating calving fronts but also of grounded ice walls. Timewise, we refer to first (1997-2008) and second (2009-2018) decade even though the time periods are 11 and 9 years, respectively, limited by the availability of coastline products. The first coastline product was automatically extracted from the high-resolution Radarsat-1 mosaic by adaptive thresholding and finalized by manual correction (Liu and Jezek, 2004). The Radarsat-1 mosaic imagery was acquired between September and October 1997 with a spatial resolution of 25 m. The entire dataset is freely available at the National Snow and Ice Data Center (NSIDC) (1997). Glacier and ice shelf fronts for the year 2009 were manually delineated from the MOA 2009 Surface Morphology Image Map acquired during austral summer 2008/2009 (Nov-Feb) with a spatial resolution of 125 m (Scambos et al., 2007). This dataset is also freely available at NSIDC (2009). The coastline for 2018 was automatically extracted via a fully convolutional network from Sentinel-1 mid resolution (40 m) dual-pol imagery (see methods section).

2.2 ERA 5

We use ERA5-Land monthly averaged atmospheric re-analysis data for air temperature and snowmelt information. It is the most state-of-the-art reanalysis product from the European Centre for Medium-Range Weather Forecasts (ECMWF) replacing the former ERA-Interim product. Data is available from 1981/82 to today at a 9 km spatial resolution. As ground-based meteorological observations are scarce over the Antarctic continent we decided to use the reanalysis data even though modelled data is less accurate compared to in-situ measurements. Studies comparing in situ observations to modelled data prove that ERA5 surface air temperature (2 m temperature) outperforms the former ERA-Interim product. ERA5 temperature data has the ability to capture annual variability and magnitude of temperature change over the Antarctic Ice Sheet (Gossart et al., 2019; Tetzner et al., 2019). The mean absolute error is 2.0° C with higher accuracies in the coastal areas and less accurate results in the interior of the ice sheet (Gossart et al., 2019). Tetzner (2019) report much higher accuracies for the Antarctic Peninsula with a mean absolute error of -0.13° C. Compared to the mean, the variability of temperature is captured with high accuracy at a mean Pearson correlation coefficient of 0.98 (Gossart et al., 2019; Tetzner et al., 2019). We divided temperature measurements into the cooler half ("winter" Apr-Sep) of the year and warmer half ("summer" Oct-Mar) to separate the environmental forcing for different seasons.

Snowmelt data should be handled with care as accuracy assessments for the ERA5 Land snowmelt product were not yet performed. Surface mass balance (SMB) data including modelled snowmelt data was found to slightly underestimate the

https://doi.org/10.5194/tc-2020-224
Preprint. Discussion started: 21 September 2020

SMB (Gossart et al., 2019). Snowmelt is calculated within the summer months December, January and February where most melt occurs. The amount of snow melt is calculated in mm water equivalent (mm w. eq) per day.

For zonal (West to East) wind speed estimations we use ERA5 monthly averaged data at 10 m above the surface with a resolution of approx. 31 km. ERA-5 captures the spatial variability of near-surface wind speed but underestimates strong winds and coastal winds whereas the wind speed over the interior is captured very accurately especially during summer. Over the ocean, ERA5 annual mean zonal wind speed is considerably underestimated compared to ASCAT (Advanced Scatterometer) observations (Belmonte Rivas and Stoffelen, 2019). Overall, the mean absolute error over the continent is 2.8 m/s with high variance in space and time but an accurate representation of the annual variability (Gossart et al., 2019). ERA5 data is freely available at the Copernicus Climate Change Service Climate Data Store (CDS) (C3S, 2017). Zonal Wind was calculated for the summer months (DJF) because especially easterly winds show a weakening trend during summer but not throughout the entire year (Hazel and Stewart, 2019).

2.3 Sea Ice Days

The most recent Global Sea Ice Concentration Climate Data Record (Version 2) (Lavergne et al., 2019) was downloaded from the Ocean and Sea Ice Satellite Application Facility (Osisaf, 2020). We used the daily product (OSI-450, OSI-430-b) during sea ice months April through October. The product covers the time period 1982 to 2018 and is derived from passive microwave data by Nimbus 7 and DMSP satellites. The final sea ice concentration is computed by the passive microwave data in combination with ERA-Interim data. The standard deviation of mismatch between OSI products and ice chart analysis on sea ice concentration is 8 % for ice and open water during winter (JJA). The trend in sea ice extent is very similar between OSI and ice chart products (Brandt-Kreiner et al., 2019) which allows the assumption of a very accurate data set. The product has a resolution of 25 km x 25 km. In order to calculate actual sea ice days we count each pixel per day with a sea ice concentration higher 15 % as suggested by previous studies (Miles et al 2016, Massom et al 2013). Especially in the early acquisition years data gaps occur and second-daily acquisitions exist until mid of 1987. In this case, we multiplied the monthly available sea ice days by the proportional amount of missing days. We decided not to use data for the year 1986 as data for entire months were missing and mean sea ice days per year could not be calculated accurately.

2.4 Sea Surface Temperature

Sea surface temperature measured by satellite sensors is also provided by the CDS (C3S, 2017). The most up-to-date product Level 4 (Version 2) consists of multiple satellite observations from NOAA, ERS, Envisat and Sentinel-3 satellites with a 0.05 ° gridded resolution (approx. 5.5 km). We calculated surface temperatures only for months with little to no sea ice cover (Oct-Mar). This reduces errors over sea ice where the thickness and concertation of sea ice can account for large measurement errors (Kwok and Comiso, 2002). Uncertainties of Level 4 data vary depending on the year of acquisition and latitude of measurement. The median difference compared to in-situ drifter measurements is up to -0.4 K for low latitudes during the early acquisition years before 1996. Afterwards the accuracy increases to better than -0.1 K for low latitudes. A

https://doi.org/10.5194/tc-2020-224
Preprint. Discussion started: 21 September 2020

The Cryosphere Discussions

stability assessment of the Level 4 product calculated a maximum trend of 0.01 K per year (Embury, 2019). A summary of all processed climate variables is given in Table 1.

Table 1 Summary of processed climate variable data sets.

Climate Variable	Time Span	Season	Spatial Resolution	Accuracy	Data	Data Store
Air Temperature	1982-2018	Summer (Oct-Mar) Winter (Apr-Sep)	9 km	0.13 – 2.0 °C	modelled	CDS
Snow Melt	1982-2018	Dec-Feb	9 km	-	modelled	CDS
Zonal Wind	1982-2018	Dec-Feb	31 km	2.8 m/s	modelled	CDS
Sea Ice Days	1982-2018 (not 1986)	Apr-Oct	25 km	8 % std to ice chart	modelled + satellite	Osisaf
Sea Surface Temperature	1982-2018	Oct-Mar	~5.5 km	-0.1 to -0.4°C	multiple satellites	CDS

3 Method

3.1 Extraction of Sentinel-1 Coastline

We use a modified version of the automatic coastline extraction approach published by Baumhoer et al. (2019) to extract the Antarctic coastline for 2018. To cover the entire Antarctic coastline, 158 dual-pol and 17 single-pol medium resolution Sentinel-1 scenes were processed. Dual polarized scenes contain radar backscatter values for the polarizations HH and HV whereas single polarized scenes only include the HH polarization. The coastline was split into 18 zones based on ice flow divides, defining major ice sheet basins after Rignot et al. (2011). For each zone all available scenes acquired during winter months (June, July, August) in 2018 were selected. Depending on the scene availability, each zone was covered at least by one Sentinel-1 scene and in the best case by three scenes. In case no dual-pol scenes were available single-pol data was selected. First, each scene was pre-processed (thermal correction, calibration, terrain correction), masked with a coastline buffer of 100 km and tiled into 780x780 pixel tiles. The convolutional neural network (CNN) U-Net was used to segment each tile into the class ocean and the class land ice. We trained the U-Net on 15 different Antarctic coastal regions during various seasons with 40,036 image tiles from 75 Sentinel-1 scenes. For single-pol scenes we re-trained our network for HH polarized images only. This decreased the accuracy slightly as only one polarization limits the information on surface backscatter characteristics. In the post-processing step the mean of all segmented tiles within one zone was calculated and then thresholded by a prediction probability of 50 % for the class land ice. In case of multi-coverage by several satellite scenes more robust results were obtained by merging the prediction probabilities. Morphological filtering and the exclusion of higher ice sheet areas by integrating elevation information from the TanDEM-X Polar DEM 90 reduced further errors. Finally, from the binary segmentation results the border between both classes was extracted as the final coastline.

https://doi.org/10.5194/tc-2020-224
Preprint. Discussion started: 21 September 2020

3.2 Derivation of Calving Front Change

Calving front change was estimated by calculating the change in area between the coastlines in 1997, 2009 and 2018 over the area of glaciers and ice shelves. As coastline extraction and delineation is a very subjective task and all coastlines originated from different sources and resolutions deviations in many areas occurred. Especially areas of fast ice, mélange and icebergs trapped in sea ice were error sources. For the automatically extracted coastline 2018, errors existed along the western Antarctic Peninsula and in areas where only single-pol imagery was available. The MODIS derived coastline often included snow covered sea ice which is difficult to distinguish from glacier ice in optical imagery. To minimize errors and mismatches all three coastlines were manually corrected and adjusted. Each coastline product was corrected based on the satellite imagery from which they were originally created. After manual correction any change in area between the coastline products could be attributed to glacier front change. From each coastline a raster (resolution 40 x 40 m) was created with a unique value over the ice covered area. All three raster layers were stacked and summed up, so each raster value pixel is associated with retreat or advance of the specific year. The area change was calculated for each major floating ice shelf and glacier wider than 3 km based on a 40 m resolution raster in Polar Stereographic Projection. To account for inaccuracies in the manual adjustment of all coastlines, we measured the accuracy as the area change over 30 randomly picked stable coastline areas. Any change over those regions can be attributed to errors in manual delineation, imagery resolution differences and errors in orthorectification of the different satellite image mosaics. The error is calculated per km of the coastline and calculated in proportion to the actually measured front length. On average, the coastlines deviated ±1.2 pixels per kilometre per year. Broken down for each coastline product, the error between 1997-2009 was 0.4 pixels per km per year, 2.3 pixels between 2009-2018 per km per year and 0.9 pixels between 1997 -2018 per km per year.

3.3 Climate Data Correlation

In order to assess the influence of climate variables (such as air temperature, sea ice days, sea surface temperature, snowmelt and zonal wind) on glacier and ice shelf retreat, we spatially correlated the percentage of advance and retreat for each minor glacier basin (as defined by Mouginot (2017)) with the decadal mean value of each climate variable. Means were calculated from 37-years of climate data for the time periods 1997-2008, 2009-2018 and 1982-1996. Hence, the inputs of the correlation covered the two time spans 1997-2008 and 2009-2018 for which also the glacier retreat was calculated. To also assess relative changes in the variables to previous times we subtracted the long-term mean (1982-1996). Zonal wind, sea ice coverage and sea surface temperature means were calculated within a 100 km seawards buffer along the coastline. Mean air temperature and snowmelt was calculated within a 100 km buffer landwards from the coastline covering the surface of ice shelves. Again also relative values were calculated by subtracting the long-term mean 1982-1996. To remove the effect of different basin sizes and different amounts of ice discharge we took the percentage of advance and retreat within each basin instead of the absolute value for the correlation. Input data for the Pearson correlation were the mean of all assessed climate variables (absolute and relative averages) as well as the percentage of retreat and advance. This created 14 different variables

https://doi.org/10.5194/tc-2020-224
Preprint. Discussion started: 21 September 2020

The Cryosphere Discussions
Open Access
EGU

which were correlated with each other based on 188 observations (N=188). The number of observations composes from 94 assessed glacier basins with variable averages for two different decades (1997-2008 and 2009-2018).

4 Results

4.1 Advance and Retreat of Antarctic Glaciers and Ice Shelves

Circum-Antarctic glacier and ice shelf front changes were assessed by comparing Antarctic coastline products during 1997-2008 and 2009-2018. The results are visualized in Figure 2. Between 1997 and 2008 ice shelf and glacier extents decreased by -29,618±29 km^2 where 69 % of the total area retreated and 31 % advanced (see Table 2 for all change rates). In contrast, during the period 2009 to 2018 a slight area increase of 7,108±144.4 km^2 could be observed with 44 % of the total area retreating and 56 % advancing. The locations of area change are almost similar for both observation periods. Ice shelves along the Antarctic Peninsula retreated over the entire observation period (1997-2018). The only exception was the advance of the Larsen D Ice Shelf which is located close to the Ronne Ice Shelf in the Weddell Sea (see Figure 2). Especially between 1997 and 2008 huge disintegration events of the Larsen B, Wilkins and Wordie Ice Shelf resulted in a 37 % higher calving amount at the Antarctic Peninsula as during 2009-2018. During the second decade the breakup of iceberg A-68 from the Larsen C Ice Shelf and the further disintegration of the Wilkins Ice Shelf were hotspots of strong area loss. In total, the rate of retreat along the Antarctic Peninsula was 5-6 times higher than glacier advance over the last 20 years.

Table 2 Retreat and advance rates of Antarctic glaciers and ice shelves for each basin between 1997 and 2018 (upper table). Total lost and gained ice shelf/glacier area per decade (lower table). For basin abbreviations see Figure 2.

		1997-2008		2009-2018		1997-2018	
	RATES	advance (km^2/yr)	retreat (km^2/yr)	advance (km^2/yr)	retreat (km^2/yr)	advance (km^2/yr)	retreat (km^2/yr)
EAIS	A-Ap	249±2.5	164±2.5	295±14.5	112±14.5	215±5.4	85±5.4
	Ap-B	62±0.8	89±0.8	80±4.7	53±4.7	34±1.7	36±1.7
	B-C	187±0.3	4±0.3	186±1.8	20±1.8	179±0.7	4±0.7
	C-Cp	380±1.3	167±1.3	363±7.5	153±7.5	323±2.8	111±2.8
	Cp-D	49±0.8	58±0.8	45±4.5	97±4.5	23±1.7	51±1.7
	D-Dp	154±0.8	64±0.8	156±4.8	317±4.8	85±1.8	111±1.8
	Dp-E	68±1.6	58±1.6	74±9.2	81±9.2	34±3.4	32±3.4
	E-Ep	6±0.5	411±0.5	156±2.9	8±2.9	5±1.1	154±1.1
	Jpp-K	163±0.3	2±0.3	252±2	2±2	203±0.7	1±0.7
	K-A	306±1.3	23±1.3	285±7.5	82±7.5	270±2.8	24±2.8
	EAIS	**1626±10.3**	**1040±10.3**	**1894±59.4**	**926±59.4**	**1370±22**	**607±22**
AP	Hp-I	20±0.8	328±0.8	25±4.4	305±4.4	11±1.6	306±1.6
	I-Ipp	87±0.7	938±0.7	59±3.8	592±3.8	12±1.4	715±1.4
	Ipp-J	91±0.8	67±0.8	118±4.4	75±4.4	71±1.6	38±1.6
	AP	**198±2.2**	**1333±2.2**	**202±12.6**	**972±12.6**	**94±4.7**	**1060±4.7**
WAIS	Ep-F	160±1.3	868±1.3	452±7.4	74±7.4	136±2.8	341±2.8
	F-G	103±0.9	101±0.9	73±5.1	106±5.1	59±1.9	73±1.9
	G-H	40±0.6	371±0.6	49±3.5	369±3.5	14±1.3	340±1.3
	H-Hp	26±0.6	35±0.6	6±3.6	97±3.6	3±1.3	51±1.3
	J-Jpp	29±1	1127±1	643±5.6	26±5.6	13±2.1	317±2.1
	WAIS	**358±4.4**	**2502±4.4**	**1222±25.3**	**672±25.3**	**225±9.4**	**1121±9.4**

TOTAL	1997-2008 advance (km^2)	1997-2008 retreat (km^2)	2009-2018 advance (km^2)	2009-2018 retreat (km^2)	1997-2018 advance (km^2)	1997-2018 retreat (km^2)
WAIS	3942±7	27525±10	11612±48	6382±48	4617±38	22970±38
AP	2178±8	14660±8	1920±40	9232±40	1929±32	21722±32
EAIS	17886±11	11439±11	17990±56	8801±56	28089±45	12453±45
AIS	**24006±29**	**53624±29**	**31522±144**	**24414±144**	**34636±116**	**57146±116**
total	**-29618±29**		**7108±144**		**-22510±116**	

The West Antarctic Ice Sheet (WAIS) lost more than three-times as much calving area in the first decade (1997-2008) compared to 2009-2018. 75 % of West Antarctic glacier and ice shelf retreat were caused by Ronne and Ross West Ice Shelf during the first decade. The retreat at WAIS was significantly lower in the second decade whereas Ross and Ronne Ice Shelf started to advance again. A different pattern occurs when considering West Antarctic calving front change without Ronne and Ross Ice Shelf. Then the glacier and ice shelf retreat during both observation periods is predominant. Pine Island and Thwaites glacier retreated over the entire observation period (1997-2018). Getz and Abbot Ice Shelf had stable front positions within the first decade but started to retreat since 2009. Only Crosson Ice Shelf showed a contradicting pattern with retreat in the first and re-advance in the second decade.

The glaciers and ice shelves of the EAIS showed an overall stable advancing tendency with similar rates for both decades with slightly more retreat during the first and slightly more advance during the second decade. Strongest advance was observed for Amery and Filchner Ice Shelf as well as at the shelves at Dronning Maud Land and Queen Mary Land. During 1997-2008, clear retreat appeared for Ross East Ice Shelf and along Enderby Land especially at Shirase Bay. Wilkes Land as well as Victoria Land had an almost equal share of retreat and advance. Between 2009 and 2018 Ross Ice Shelf and Enderby Land entered a phase of advance whereas Wilkes Land, George V and Adélie Land started to retreat predominately.

https://doi.org/10.5194/tc-2020-224
Preprint. Discussion started: 21 September 2020

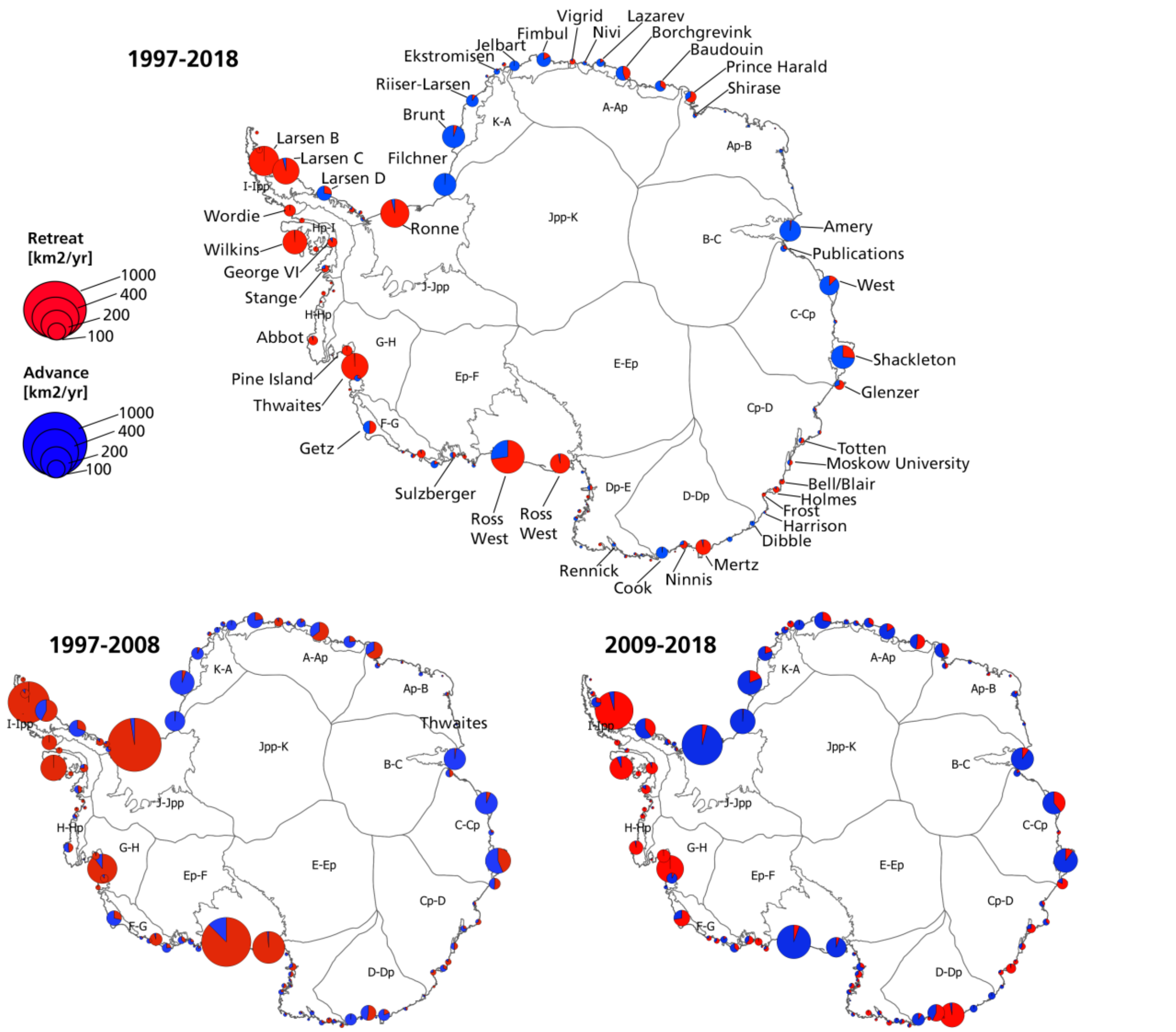

Figure 2 Glacier and ice shelf extent changes for major glaciers and ice shelves over the last two decades. Circles indicate the rate of retreat or advance. Major ice sheet basins as defined by Rignot et al. (2011).

4.2 Air Temperature

The mean Antarctic air temperature was equal for both decades during winter but in summer +0.6 °C higher in the second decade (2009-2018). But the overall mean does not reflect the strong regional differences in air temperature changes as shown in Figure 3. During summer and winter the Antarctic Peninsula and the adjoining coast along Bellingshausen and Amundsen Sea as well as Queen Mary Land were cooler between 2009-2018 whereas the interior of the ice sheet warmed during this period. Compared to the long-term mean (1982-1996) summer temperatures between 1997-2008 were cooler

https://doi.org/10.5194/tc-2020-224
Preprint. Discussion started: 21 September 2020

except for the Peninsula, Queen Mary Land, Ross West and Filchner Ice Sheet. In the second decade this changed in sign where the Antarctic Peninsula started to cool down and the interior increased in temperature. For the winter months almost over the entire Antarctica continent a warming tendency was observed compared to the long-term mean. Only exceptions were Victoria, Oates and George V Land. Additionally, over Getz Ice Shelf cooler temperatures of 1°C occurred in 2009-2018 compared to the long-term mean. For Dronning Maud Land a strong change was observed as the ice shelf surfaces warmed up to 1.8°C in the second decade.

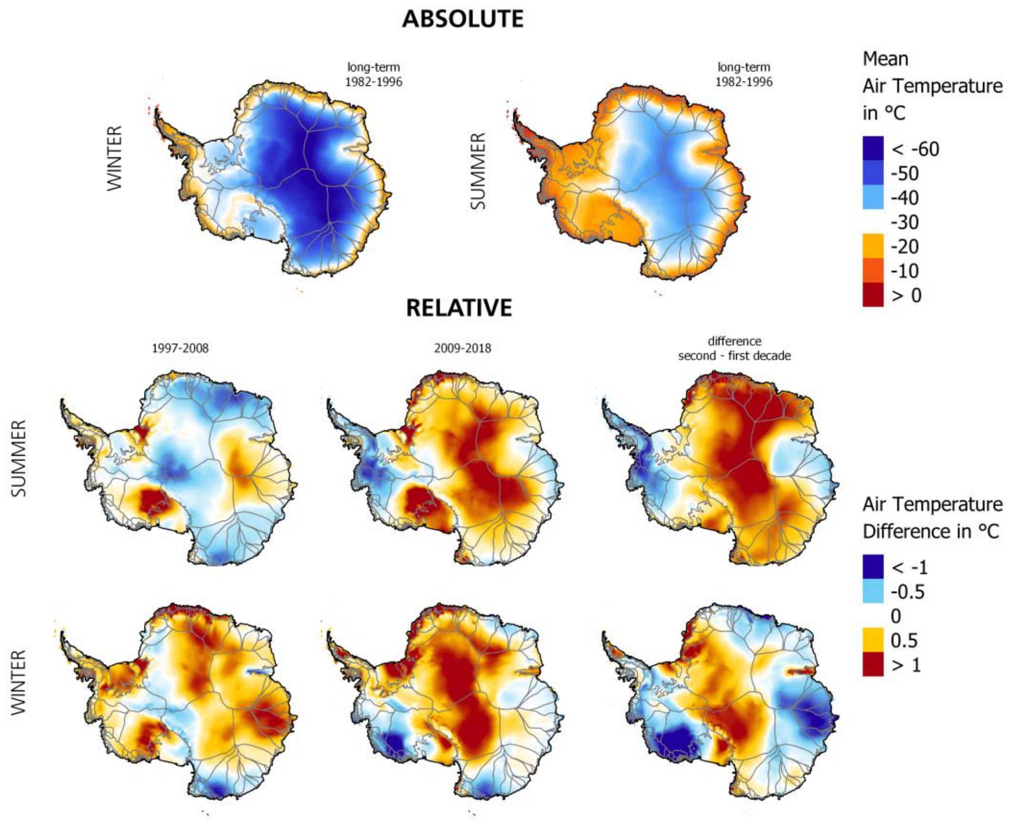

Figure 3 Absolute long-term air temperature and relative changes compared to the long-term mean. Additionally the difference between the first and second decade is illustrated.

4.3 Sea Ice Days

A decrease or increase in sea ice days refers to the difference in the number of sea ice days per year (during the sea ice season April to October) compared to the long-term mean. The strongest decrease in sea ice days could be observed at the northern tip of the Antarctic Peninsula with a shorter sea ice cover per year of up to 40 days during the first decade compared to the long-term mean. During 1997 and 2008 a decrease in sea ice days was observed along the Bellingshausen Sea with up to 20 days less and in the Amundsen Sea with up to 5-10 days less. Compared to the first decade, the mean sea ice cover persisted longer in the second decade along the Antarctic Peninsula and the Bellingshausen Sea whereas in the Amundsen

Sea the sea ice days decreased up to 10 days further compared to the first decade. Along the EAIS, sea ice coverage increased 10 days on average except for Dronning Maud Land with a slight decrease of up to 5 days. When comparing the two decades more sea ice days occurred during 2009 to 2018 along the EAIS and the northernmost Antarctic Peninsula whereas the decrease along West Antarctica continues. Changes in sea ice days were less extreme along East Antarctica with ±10 days in difference compared to 1982-1996. Between 1997-2008 the duration of sea ice cover was up to 5 days shorter along Dronning Maud and Wilkes Land compared to the long-term mean. In the second decade sea ice days along the entire EAIS increased with a highest increase along Wilkes Land with up to 10 days (compared to 1982-1996). The described changes in sea ice days are visualized in Figure 4.

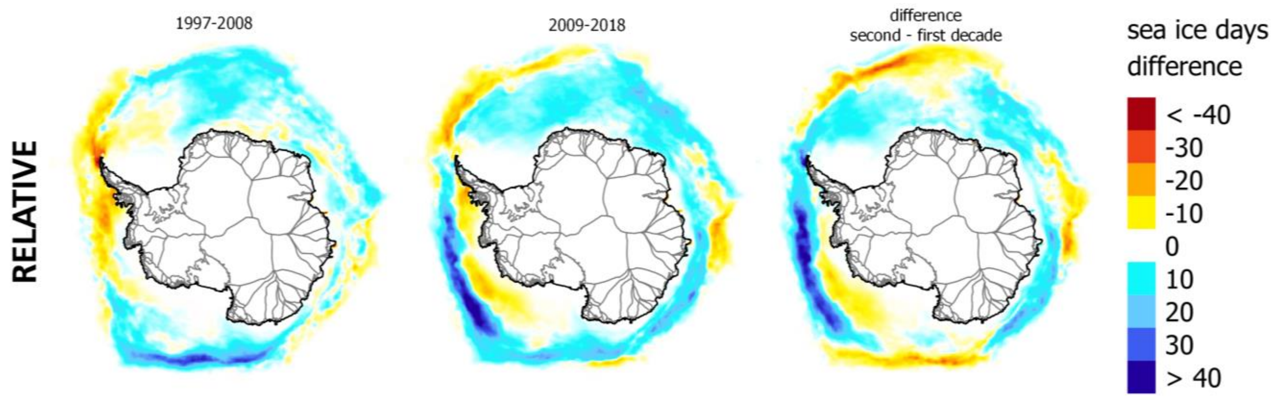

Figure 4 Difference in the number of sea ice days per year (during the sea ice season April to October) compared to the long-term mean (1982-1996) and the difference in sea ice cover duration between both decades.

4.4 Sea Surface Temperature

The changes in sea surface temperature during months with little sea ice cover (October to March) relative to the long-term mean are shown in Figure 5. Sea surface temperatures of the southern ocean cooled (~ -0.5°) along the EAIS and warmed along WAIS and the western Antarctic Peninsula (~ +0.5°C) within the last two decades compared to 1982-1996 which is above the data uncertainty of 0.1 to 0.4 K. The warming was less strong in the first decade and intensified within the second decade especially in the Bellingshausen Sea with maxima at George VI north (+0.65°C) and Pine Island Bay (+0.35°) with a slightly weaker increase along the Amundsen Sea (+0.15°C). The cooling along the East Antarctic was less strong in the second decade. Along East Antarctica for Amery Ice Shelf (+0.35°C), West Ice Shelf (+0.2°C) and Shackleton Ice Shelf (+0.25°) warming was observed compared to the first decade.

https://doi.org/10.5194/tc-2020-224
Preprint. Discussion started: 21 September 2020

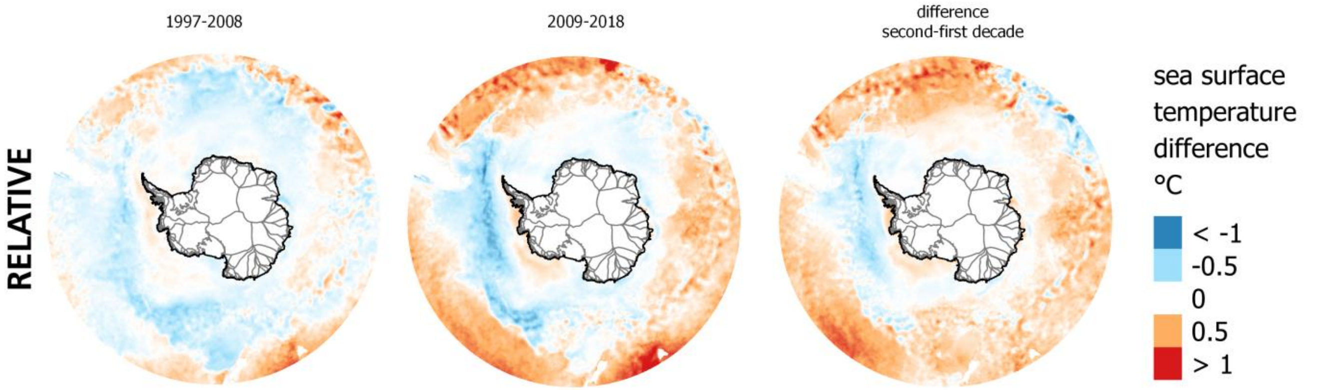

Figure 5 Mean sea surface temperature changes (October to March) compared to 1982-1996 and the difference in sea surface temperatures between both decades.

4.5 Snowmelt

Snowmelt over the Antarctic Peninsula was more extensive during the long-term mean compared to the recent two decades. This is the reason why relative snowmelt in 1997-2008 and 2009-2018 was mostly negative with up to -0.3 mm w. eq. per day (see Figure 6). Nevertheless, strong snowmelt occurred also during the recent two decades but more selective over Wilkins and Larsen B Ice Shelf as well as at the northern tip of the Antarctic Peninsula. During the long-term mean, snowmelt concentrated on the Antarctic Peninsula, Ronne, Abbot, Shackleton and Amery Ice Shelf as well as Shirase Bay. In the first decade snowmelt expanded to Pine Island Bay, Getz Ice and Ross Ice Shelf as well as along Wilkes, George V and Dronning Maud Land. In all cases, the increase in melt was small with 0.1 mm w. eq. per day. Within the most recent decade melt got more extensive (+0.1 mm w. eq. per day) over George V, Oates and parts of Wilkes Land as well as over Getz and Sulzberger Ice Shelf. Melt peaks in Pine Island Bay and Dronning Maud Land could only be observed during the first decade.

4.6 Zonal Wind

The Antarctic continent is circled by weak and irregular easterly winds driven by high pressure areas over the interior of the Antarctic continent created by cold and dry air. In case of a positive Southern Annular Mode (SAM) the easterlies weaken and the west wind drift shifts poleward. A positive SAM occurs when air pressure over the Antarctic Ice Sheet lowers but rises over the subtropical ocean. In the first decade, weakening easterlies (~ +0.5 m/s) were observed along the Antarctic Peninsula, Bellingshausen and Amundsen Sea as well as in East Antarctica in the area of Shackleton Ice Shelf. Stronger easterlies occurred only at George V and Dronning Maud Land. Within the second decade the strengthening westerlies along East Antarctica expanded from Amery Ice Shelf to Victoria Land with up to + 1m/s. Also the westerlies strengthened at Bellingshausen Sea but weakened in the Amundsen Sea (see Figure 7). Strong dominating easterlies occurred along Dronning Maud Land with up to -0.75 m/s within the second decade.

https://doi.org/10.5194/tc-2020-224
Preprint. Discussion started: 21 September 2020

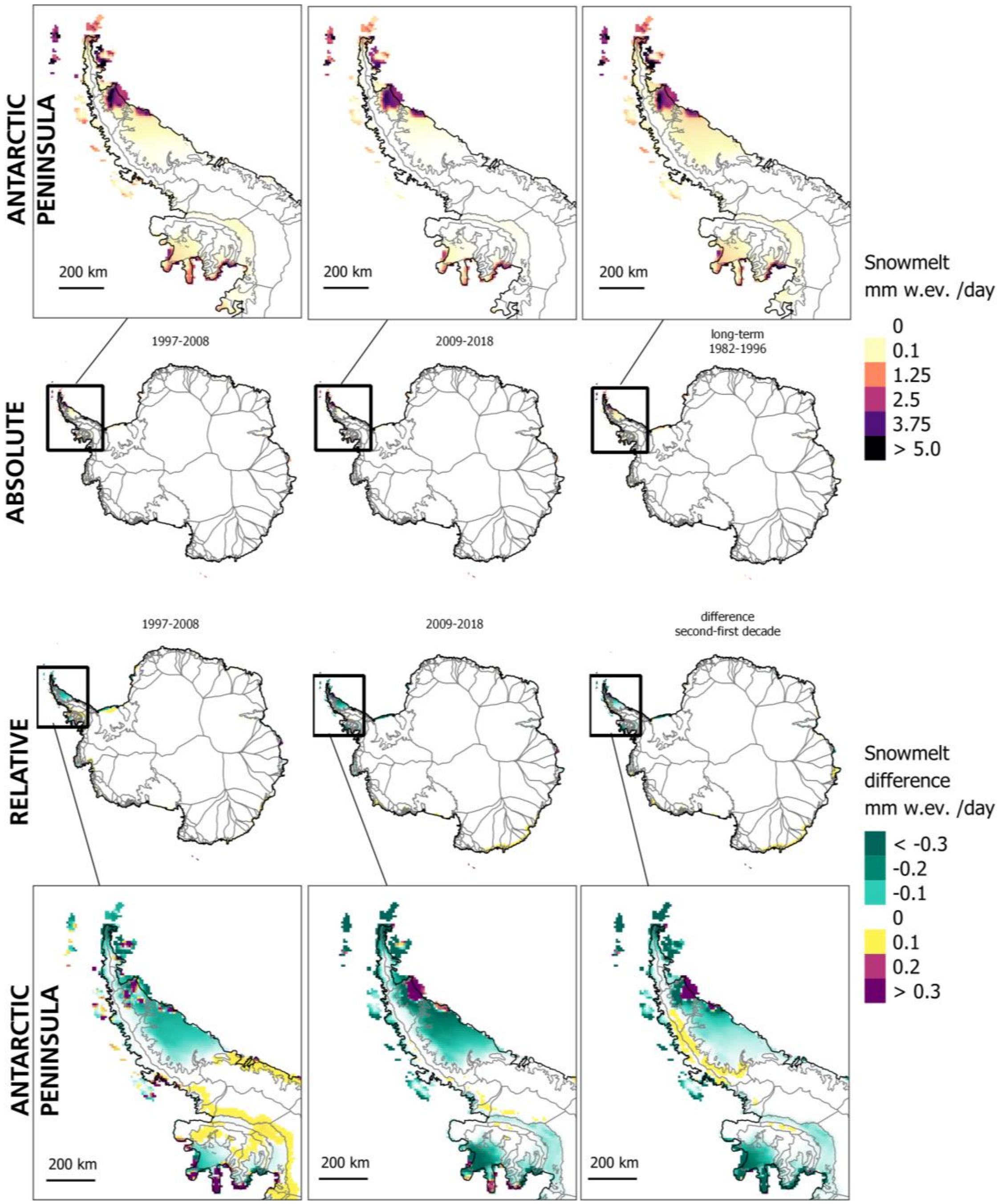

290

Figure 6 Mean snowmelt over Antarctica with enlarged views of the Antarctic Peninsula. Snowmelt is given in mm water equivalent per day.

https://doi.org/10.5194/tc-2020-224
Preprint. Discussion started: 21 September 2020

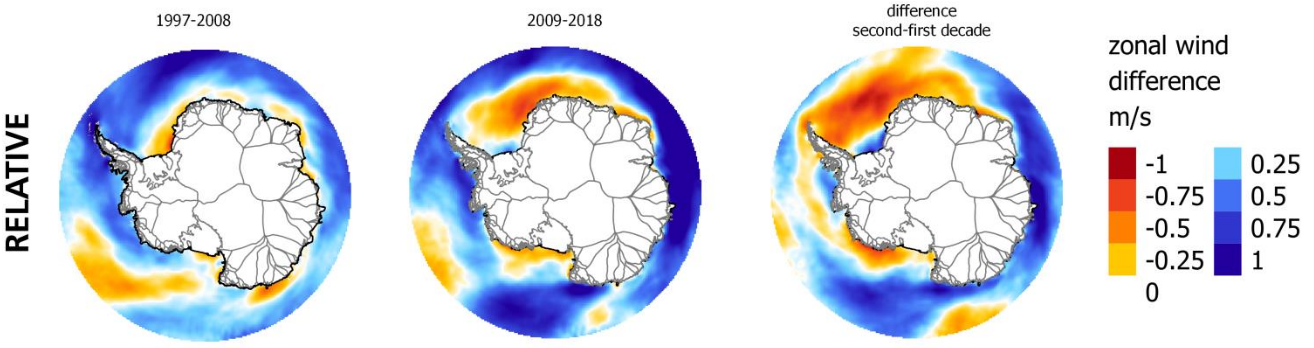

Figure 7 Zonal Wind (West to East) around the Antarctic continent in m/s for 1997-2008 and 2009-2018 compared to the long-term mean. Additionally, the difference in wind speed between both decades is illustrated. Positive shifts in zonal wind indicate stronger westerlies with the potential to cause upwelling of warm Circum Polar Deep Water (CDW).

4.7 Correlation between Climate Variables and Calving Front Retreat

Potential drivers of calving front retreat were identified by correlating the analysed climate variables with the percentage of retreat/advance within each glacier/ice shelf basin. The results of the Pearson correlation are displayed in Figure 8. Dark blue colors indicate a strong positive, dark red color a strong negative correlation. Stars indicate a significant Pearson correlation with stars for p=0.05 (*), 0.01 (**) and 0.001(***). Correlations for retreat and advance are counterparts, hence correlations are of the same magnitude for each climate variable but with reversed sign. Overall, weak to moderate correlations with significance occur for relative summer sea surface temperature, absolute air temperature, snowmelt, relative zonal wind speed and sea ice days. The strongest positive linear relationship (r=0.44) exists between calving front retreat and relative sea surface temperature. Slightly weaker is the positive correlation between glacier and ice shelf front retreat and absolute air temperature on the ice shelf surface (r_{summer}=0.18, r_{winter}=0.23). A relatively more positive zonal wind (hence strengthening westerlies) correlates positively with calving front retreat (r=0.30) but the absolute strength of zonal winds does not. Decreases in sea ice days correlate positively with calving front retreat (r_{abs}=0.33, r_{rel}=0.27). The mean daily amount of snowmelt correlates weakly but significant with glacier and ice shelf front retreat (r=0.17). The correlation of the climate variables among each other reflects that they are closely linked to each other. Higher air (r_{summer}=-0.26, r_{winter}=-0.36) and sea surface temperatures (r=0.44) have a negative relationship to an increase in sea ice days. An increase in sea ice days negatively correlated with an increase in zonal winds (r=0.31). Stronger snowmelt correlates positively with warmer summer (r=0.46) and winter (r=0.37) air temperatures. An increase of zonal winds was positively related to decreasing summer air temperatures (r_{summer}=-0.31).

https://doi.org/10.5194/tc-2020-224
Preprint. Discussion started: 21 September 2020

The Cryosphere Discussions

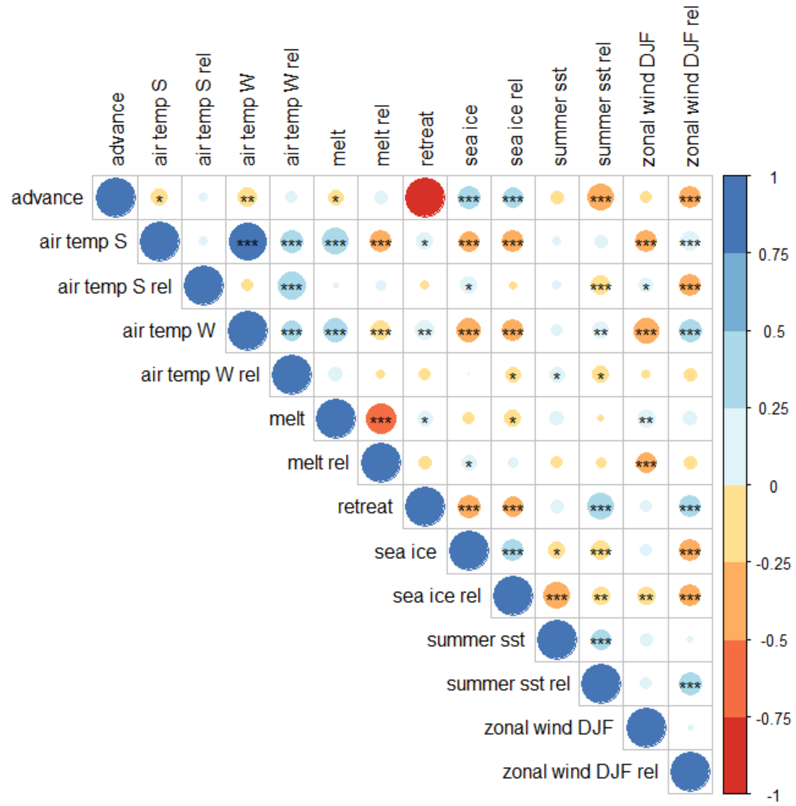

Figure 8 Correlation between glacier and ice shelf change and the analysed climate variables winter/summer air temperature, snowmelt, sea ice days, summer sea surface temperatures and zonal wind speed. Colour and circle size indicate the correlation coefficient. Stars indicate significance levels for p=0.05 (*), 0.01 (**) and 0.001(***). S: summer, W: winter, rel: relative to 1982-1996, DJF: Dec-Feb.

5 Discussion

The results section presented changes in ice shelf and glacier front extent over the last two decades in combination with environmental change. The correlation between glacier retreat and climate variables identified strengthening westerlies, higher air temperatures, intense snowmelt, a decrease in sea ice cover and rising sea surface temperature as potential drivers for calving front retreat. But a significant correlation between calving front retreat/advance and climate variables cannot alone provide conclusive evidence of a causal link. One very obvious example would be the significant correlation between calving front retreat and air temperature. This means that in coastal sectors with warmer air temperatures glacier and ice shelf retreat prevails. But from that, we cannot conclude that warmer air temperatures cause glacier retreat. It just reflects the given fact that air temperatures over the Antarctic Peninsula and West Antarctica are higher than at the EAIS but still calving front retreat along the cooler EAIS exists (see Figure 3). If rising air temperatures were able to force calving front retreat also relative changes in air temperature would have correlated with calving front retreat. As this was not the case we conclude that other drivers than air temperature forced glacier retreat over the last two decades. To find solid evidence for drivers of glacier and ice shelf retreat we will discuss observed glacier/ice shelf retreat in combination with measured changes in climate variables and scientific publications.

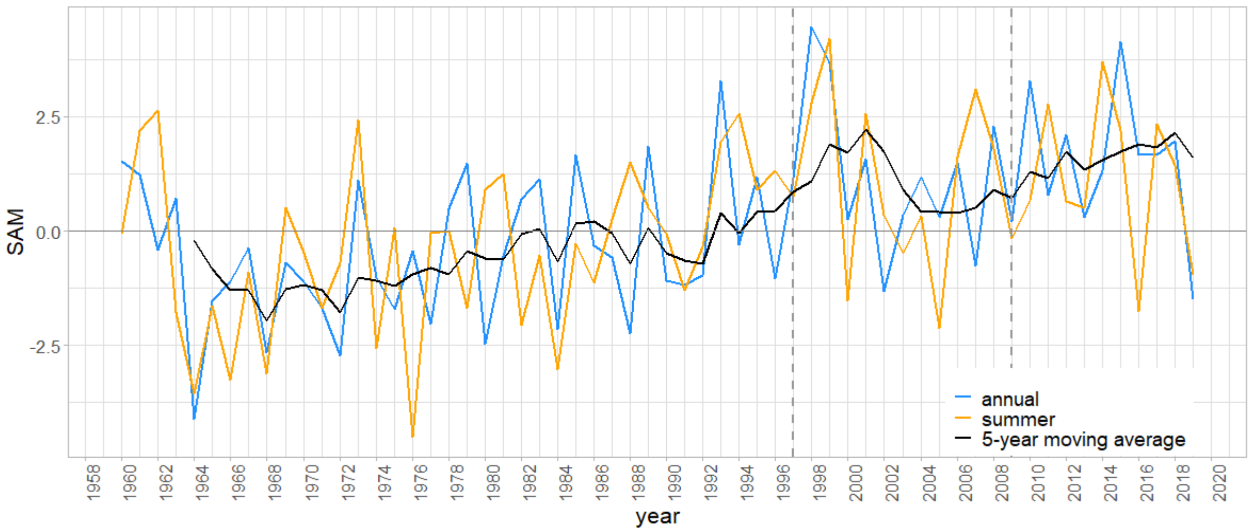

Figure 9 Southern Annular Mode (SAM) since 1960. Values are given for the annual SAM (blue), SAM during summer (orange) and a 5-year moving average for the annual SAM (black). The dashed grey lines indicate the investigated periods 1997/08 and 2009/18 as delimited by the available coastline data. For SAM during summer (Dec-Feb), the beginning of austral summer (hence December) indicates the year of the peak. Data: Marshall et al. (2003).

5.1 Antarctic Peninsula

Along the Antarctic Peninsula a decrease in ice shelf extent resulted mainly by the disintegration and retreat of Larsen B, Larsen C, Wilkins and Wordie Ice Shelf. For the major calving event of Wordie between 1997 and 2008, we observed stronger zonal winds compared to the reference period (+0.62 m/s) and the most recent decade (+ 0.28 m/s) (2009-2018). This means that during the break up event the eastern wind direction weakened towards a more westerly direction. This change in wind-direction causes upwelling of warm CDW and enhances basal melt. A change in wind direction towards westerlies is linked to positive SAM years (Marshall 2007). Figure 9 shows the strengthening of the SAM since the 1960s to better assess the link between positive phases of SAM and the observed disintegration events. The highest peak of SAM occurred during summer 98/99. This coincides with a major calving event of Wordie Ice Shelf reported by Friedl et al. (2018) for the same year. A later calving event was also associated with upwelling of warm CDW which was especially strong in the years 2008 to 2011 due to an exceptionally positive SAM (Walker and Gardner, 2017). The strong basal melt at Wordie Ice Shelf was also reported by Rignot et al. (2013) and Depoorter et al. (2013). In addition, to the continuous thinning by basal melt, it should be pointed out that the retrograde bed in a subglacial deep trough destabilized the Wordie Ice Shelf and led to grounding line retreat in 2010/2011 (Friedl et al., 2018). So far, the decreasing sea ice coverage (-14 days compared to the long-term mean) at Wordie Bay has not been discussed. We suggest that the decreased sea ice cover

https://doi.org/10.5194/tc-2020-224
Preprint. Discussion started: 21 September 2020

additionally destabilized the floating ice tongues. Similarly, also for the Wilkins disintegration during the first decade we observed similar enhanced summer zonal winds with a 0.47 m/s higher mean than compared to the reference period. Additional factors include a decrease in sea ice days (-9 days) and 0.13°C warmer sea surface temperatures and a slight increase in snowmelt by 0.06 mm w. eq. per day in the first decade compared to 1982-1996. Wilkins also experienced a calving event in 1998 (Cook and Vaughan, 2010) which overlaps with a positive SAM peak. The enhanced westerly winds suggest that also Wilkins Ice Shelf has weakened due to upwelling CWD. For a second break up event in 2008, snow melt was found to be the cause for retreat (Scambos et al., 2009). We observed only a very slight increase in snowmelt, weaker than the other described forcing factors. Either the ERA5 melt data is too inaccurate and coarse in resolution for assessing melt on single ice shelves or peak events in snowmelt have strong forcing effects on ice shelf retreat which are not well reflected on a decadal-mean basis. It is more likely that a combination of processes has caused the disintegration of Wilkins Ice Shelf. For example, a second calving event in 2009 during winter could not be attributed to melt. Rather bending stresses through variable ice thickness (Braun et al., 2009) and strong winds (Humbert et al., 2010) are likely candidates.

During the disintegration of Larsen B in 2002, zonal winds were +0.33 m/s stronger compared to the long-term mean and melt rates were high with up to 5 mm w. eq. per day but in most areas lower than during 1982-1996. Again, during the disintegration period a substantial positive SAM anomaly was recorded in summer. Positive SAM years with stronger westerlies are not associated with upwelling at the Larsen Ice Shelfs but with warm air temperatures in combination with warm winds and surface melt (Rack and Rott, 2004). Recent studies found out that increases in foehn days in a series of years related to positive SAM phases significantly increase melt (Cape et al., 2015; Leeson et al., 2017). This increases supraglacial lake formation and lake drainage which was indeed observed before the disintegration of Larsen B. But whether lake drainage is a cause or effect of ice shelf break up remains unclear (Leeson et al., 2020).

In the period of Larsen C break up, we observe lower amounts of melt (-0.2 mm w. eq. per day) compared to 1982-1996. Zonal winds were slightly more positive with +0.1 m/s compared to the reference time period but still lower than between 1997-2008 (+0.54 m/s). This might strengthen the hypothesis of a natural calving event (Hogg and Gudmundsson, 2017). Nevertheless, slight negative thickness changes were observed by Paolo et al. (2015) between 1994 and 2012, possibly indicating a future weakening of the Larsen C Ice Shelf. Larsen D forms the only exception of the strong retreating trend along the Antarctic Peninsula. This ice shelf neither experienced melt nor positive trends in zonal winds. Positive thickness changes indicate so far no potential weakening through basal melt (Paolo et al., 2015). The mass balance of Larsen D-G is, depending on the study, positive (Gardner et al., 2018) to slight negative but still much smaller than the huge negative mass balance of the rest of the Antarctic Peninsula (Rignot et al., 2019). Geroge VI and Stange Ice Shelf were relatively stable during 1997 to 2008 and started to retreat in 2009-2018. Slightly strengthening westerlies (+0.25 m/s) but almost no melt (0.02 mm w. eq. per day) occurred. Summer sea surface temperatures increased by +0.62°C and +0.38°C for George VI south and Stange ice shelves in the second decade compared to the reference period. Both ice shelves started to double the retreat rate during the second decade compared to the first. George VI is not believed to disintegrate rapidly (Holt et al.,

https://doi.org/10.5194/tc-2020-224
Preprint. Discussion started: 21 September 2020

2013). But recent developments might require to reconsider this assumption because calving front retreat, recently detected supraglacial lakes on the ice shelf surface (Dirscherl et al., 2020) and moderate basal melt (Paolo et al., 2015) occurred.

5.2 WAIS

Glacier and ice shelf front retreat of the WAIS is clearly dominated at Pine Island Bay and at the biggest ice shelves Ross West and Ronne Ice Shelf lost the biggest amount through calving with -732±0.73 km^2/yr and 1,098±0.91 km^2/yr between 1997 and 2008, respectively. But compared to the sheer size of the ice shelves the amount is not exceptional. The Ross West Ice Shelf already experienced such a calving event before 1962, where the front had about the position of 2004 after the maximum extent around 1997 (Ferrigno et al., 2007). Also the maximum extent of the Ronne Ice Shelf was in 1997 and its minimum extents occurred in 1974 and 2004 (Ferrigno et al., 2005). We could neither observe a reduction of sea ice nor increases in sea surface temperature (0.02 °C) and zonal winds (-0.15 m/s). Only strong melt (0.5 mm w. eq. per day) occurred on the calving area on Ronne Ice Shelf but even higher melt occurred between 1982 and 1996 in the same area. These observations suggest a calving event within the natural calving cycle instead of a long-term forced retreat. Nevertheless, recent studies predict that the Ronne-Filchner Ice Shelf will be affected by increasing basal melt through changing sea ice conditions and wind direction in the future (Darelius et al., 2016).

Pine Island and Thwaites Glacier showed strong retreat rates with 40±0.15 km^2/yr and 288±0.77km^2/yr between 1997 and 2018. During summer both experienced strengthening westerlies with +0.28 m/s in 1997/2008 and +0.25 m/s in 2009/2018 compared to the long term reference. The only indicator Pine Islands retreat rate tripled from 97/08 to 09/18 but Thwaites Glacier retreated at the same rate is an increase in sea surface temperature. Summer sea surface temperatures raised by 0.28°C at the front of Pine Island but only 0.11°C at Thwaites Glacier form the first to the second decade. It should be mentioned that besides differences in sea surface temperature both glaciers have different bed topographies and glacier morphologies which influence their sensitivity to basal melt, land fast ice persistency and hydrofracture (Miles et al., 2020; Milillo et al., 2019; Seroussi et al., 2017; Yu et al., 2017).

In contrast to the fast retreating glaciers at Pine Island Bay, the Abbot and Getz Ice Shelf did not experience increases in sea surface temperature between the two decades (+0.13°C). Abbot is also affected by increases of westerlies by 0.24 m/s from the first to the second decade whereas Getz is not (-0.41 m/s). Abbot Ice Shelf experienced little basal melt (1.5 m/decade) until 2012 whereas Getz Ice Shelf thinned at a maximum rate of 66.5 m/decade making it the largest contributor to Antarctic ice shelf volume loss through melt (Paolo et al., 2015). The still missing retreat could be attributed to the fact that both have several pinning points stabilizing the ice shelf, the glacier flow velocities are low (Mouginot et al., 2019), no forcing by increased sea surface temperatures occurred and the bed topography is very specific. The bed below Abbot Ice Shelf is situated around -200 m with only a small trough reaching below 500 m, while the Getz Ice Shelf's bed lies like a barrier around 400 m before deepening closer to the grounding line up to 700 m. In comparison, the bed of Pine Island Glacier reaches depths around 700-1000 m (Fretwell et al., 2013).The higher beds may have protected the ice shelves more

https://doi.org/10.5194/tc-2020-224
Preprint. Discussion started: 21 September 2020

effectively from upwelling CDW in combination with stabilizing ice rises as pinning points. But when environmental conditions will further force retreat also Getz and Abbot will retreat. First signs of destabilization already occurred as for both ice shelf grounding line retreat has been found since 2008 (Chuter et al., 2017). The most stable ice shelves along West Antarctica are Sulzberger and Nickerson Ice Shelf. They experience almost no basal melt because they already belong to the cooler Ross Sea (Rignot et al., 2013) and did not experience any identified drivers of calving front retreat.

5.3 EAIS

The EAIS was long believed to represent the invulnerable part of Antarctica with a positive mass balance and healthy glaciers. Recent mass balance estimations show that East Antarctica is losing mass since 1979 with an increasing loss since 1999 (Rignot et al., 2019). This stands in contrast to altimeter measurements recording an almost stable mass balance for the EAIS since 1992 (IMBIE, 2018). This is in line with our ice shelf front changes along the EAIS, advance dominated over the last two decades with regional differences we will discuss in the following. In Victoria Land, we do not see any possible environmental forcing that could have caused glacier or ice shelf retreat. Retreat and advance is equally balanced within the entire observation period. Other authors also others found that glaciers along Victoria Land are stable (Fountain et al., 2017). Rather glacier type and topography are responsible for glacier change than climate forcing (Lovell et al., 2017). Although Oats and George V Land have experienced a negative mass balance since 1999 we cannot see a negative trend in glacier extent. The only big calving event occurred at Mertz glacier through iceberg collision (Tamura et al., 2012). During 2008-2018, Wilkes Land is the only east Antarctic basin where simultaneously several glaciers disintegrated. Miles et al. (2016) linked less sea ice days to the exceptional retreat of glaciers between 2000 and 2012. During our observation period we cannot observe a connection between retreat and less sea ice days. This might be due to the fact that during 1997/08 sea ice days were only ~ 5 days less vs. ~34 days between 2000 and 2012, as reported by Miles et al. (2016). This suggests that only extreme reductions in sea ice can be related to glacier retreat, implying that sea ice alone cannot be the only explanation for retreat along Wilkes Land. We propose that upwelling CWD weakened the glaciers by basal melt as a very strong positive tendency in zonal wind with up to +0.44 m/s was observed in the second (but not in the first) decade compared to the long-term mean. No forcing through enhanced snowmelt or increased sea surface temperatures exist. The strengthening westerlies also influenced Glenzer Glacier at the nearby Queen Mary Coast with an increase of 0.32 m/s and 1.23 m/s in the first and second decade, respectively. Glenzer Glacier retreated strongly in 2009-2018 and might continue to do so because one important pinning point got lost and an opening crevasse is visible at the ice shelf pressing against a pinning island. Interestingly, Shackleton and West Ice Shelf do not seem to be directly influenced by strengthening winds since 2009, compared to the long-term average with a plus of 0.97 m/s and 1.2 m/s, respectively. Even though, strengthening westerlies occurred in the second decade no frontal change was observed. Hence, we propose that the ice shelves started to weaken by basal melt but a longer-term forcing is necessary to show effects in frontal retreat for bigger ice shelves. Also melt occurred on the edges of both ice shelves. Strengthening zonal winds also occurred at the front of Amery Ice Shelf between 2009 and 2018 with + 0.26 m/s. Also melt increased (+ 0.23 mm w. eq. per day) on the northern part of Amery over the last two decades whereas in the southern part it decreased (- 0.1 mm w. eq. per day). The front constantly advanced but the part affected by increased melt broke off in 2019 even though Fricker et al. (2002) predicted a calving event earliest in 2025 when the calving cycle of 65-70 years would have been reached.

The area loss at Enderby Land is mostly attributed to the changes in Shirase Bay. Here, very contrasting changes appear where the Prince Harald Ice Shelf retreats and the Shirase Glacier advances and vice versa. This was already mentioned by Jezek (2002). The only forcing in this area occurred between 1997 and 2008 with an up to 1 mm w. e. melt per day over Prince Edward Ice Shelf compared to the reference period. For Shirase Glacier no increases in melt were observed. Rather the specific glacier morphology and bed topography influenced calving (Nakamura et al., 2007).

Dronning Maud Land is dominated by advance over the entire study period. During 1997/08 we see higher area losses in the eastern part which is in line with less sea ice days (- 5 days). Air temperatures warmed up to 1.78°C during winter compared to the long-term reference periodover Dronning Maud Land, but did not lead to a calving front retreat. Historical records reveal that along Dronning Maud Land phases of retreat and advance are typical with bigger break up events between 1963 and the 70s. Retreat continued until the 90s followed by a phase of advance (Kim et al., 2001; Miles et al., 2016). Also basal melt rate estimates confirm the relatively stable state of the ice shelves (Paolo et al., 2015; Rignot et al., 2013).

5.4 A Circum-Antarctic Perspective

These above examples illustrated the link between snowmelt, strengthening westerlies, decreasing sea ice days, increasing sea surface temperatures and calving front retreat. Glacier and ice shelf front retreat occurred when at least one of the mentioned drivers strengthened compared to the long-term mean. The only exceptions where drivers strengthened but no glacier/ice shelf front retreat occurred, was observed at West and Shackleton Ice Shelf. This either suggests that one decade of forcing by a single driver (in this case strengthening westerlies) does not immediately result in calving front retreat at previously healthy ice shelves. Or the forcing by zonal winds is less strong in areas where CDW upwelling is less efficient due to strong tidal forcing (Hazel and Stewart, 2019; Stewart et al., 2018) An assessment on the required length and of a driving force to cause calving front retreat would provide important insights for future break up events. Moreover, the combination of driving factors may play an important role. For example in Greenland, the combination of oceanic and atmospheric drivers had the greatest impact on calving front retreat rather than any single driver alone. Additionally, catchment wide melt and the resulting runoff had a higher impact on the retreat of Greenlandic glaciers than local air temperatures (Cowton et al., 2018). Howat et al. (2008) found that also peak events in air temperature and sea surface temperature can initialise glacier retreat and that a reversed bed slope allows more rapid retreat. In addition, the acceleration of glacier retreat in wide, overdeepened beds with a retrograde slope was also observed by Catania et al. (2018).

The absolute amount of snowmelt correlated significantly with glacier and ice shelf retreat but not relative changes in snowmelt. The detailed comparison of snowmelt with calving front retreat revealed strong melt during the decade of the break up event. Nevertheless, snowmelt was often higher during the reference period than during the actual calving event which might indicate that longer phases of melt weaken the ice shelf over a longer time period. The low resolution of melt

https://doi.org/10.5194/tc-2020-224
Preprint. Discussion started: 21 September 2020

data did not always match the actual calving front and only allowed rough estimates. Additionally no information on the accuracy of the snowmelt product is provided which makes the considered reanalysis data prone to potentially large biases. We suggest a more detailed study on glacier and ice shelf front retreat in combination with accurate high resolution surface melt data (e.g. satellite-based surface melt estimates as published by Trusel et al. (2013)) to capture all necessary surface hydrology processes and an accurate metric for snowmelt. For example, not the amount of melt but much more the effect of ponding on the ice shelf influences its vulnerability (Joughin and Alley, 2011). Also surface hydrology processes such as lake drainage occurred prior to break up events (Leeson et al., 2020) and have to be investigated further.

Relative changes in mean air temperature could not be identified as a direct driver for calving front retreat, even though increases of up to 2°C per decade were measured in some coastal areas (e.g. Dronning Maud Land, Victoria Land) which is far beyond the uncertainty of the ERA5 air temperature data. Nevertheless, the impact of air temperature cannot be entirely ignored as surface melt is closely linked to air temperature. The effect of air temperature peak events on the amount of surface melt could reveal an indirect effect of air temperature by inducing surface melt.

Changes in zonal wind were a great proxy to identify upwelling warm CWD (Spence et al., 2014). But the magnitude is still difficult to quantify. In our analysis increases in zonal winds of only 0.25 m/s over one decade was enough to induce glacier and ice shelf front retreat (but in combination with high sea surface temperatures). But only a small increase in westerlies can be enough to increase basal melt considerably because basal melt has a nonlinear relationship with ocean temperature and can quadruple by only slight ocean warming (Jenkins et al., 2018). A quantification of a threshold of zonal wind speed to create forcing is difficult since ERA5 wind speed data underestimates wind speed in coastal areas and over the ocean (Belmonte Rivas and Stoffelen, 2019; Gossart et al., 2019). Hence, the zonal wind speed from weather station measurements is probably higher and may have a more apparent effect on ice shelves. Nevertheless, ERA5 data is very consistent and accurately captures the inter-annual variability of wind speed in the Antarctic environment (Gossart et al., 2019). Therefore, it can be assumed that the large-scale effect of atmospheric circulation is accurately represented.

We also identified that the bed topography is an important factor for the strength of basal melt which is in line with the fact that grounding line retreat enhances at retrograde beds destabilizing ice shelves (Scheuchl et al., 2016). Decreasing sea ice days showed an effect on glacier/ice shelf retreat but only if the average reduction per year was on average over 10 days within the decade. This fact might become important in the future. Recently, the turning point of an increasing Antarctic sea ice extent was reached (Ludescher et al., 2019; Parkinson, 2019).

For the first time, this study revealed the link between increased sea surface temperature and calving front retreat. The measured changes in sea surface temperature were between 0.15 to 0.6°C per year which is still below the trend uncertainty stability of 0.01 K per year (Embury, 2019). The influences of warmer sea surface temperatures are twofold. Warmer sea surface temperatures lead to the melt of fast ice which destabilizes glacier margins (Larour, 2004) and could result in retreat. Another explanation proposes that warm surface water increases melt at the waterline which creates an overhanging ice cliff that is more likely to collapse (Mosbeux et al., 2020).

https://doi.org/10.5194/tc-2020-224
Preprint. Discussion started: 21 September 2020

The identified drivers of calving front retreat are closely connected to positive SAM years. A positive SAM increases sea surface temperatures and air temperatures along AP and WAIS. It also influences the sea ice cover, snowmelt and foehn effect and enhances westerly winds along the Antarctic coastline (Cape et al., 2015; Kwok and Comiso, 2002; Marshall, 2007; Tedesco and Monaghan, 2009; Verdy et al., 2006). Extreme peaks in positive SAM could even trigger ice shelf disintegration as has been shown for Wordie Ice Shelf. To conclude, glacier and ice shelf retreat will be even more likely in the future as rising greenhouse gases and ozone depletion will cause more positive phases of SAM (Paeth and Pollinger, 2010; Wang et al., 2014) and further strengthen driving forces of calving front retreat.

6 Conclusion

For the first time, we present a circum-Antarctic record of calving front changes over the last two decades. Overall, the extent of the Antarctic Ice Sheet decreased -29618±29 km^2 between 1997 and 2008 gained an area of +7108±144.4 km^2 between 2009-2018. Glacier and ice shelf front retreat concentrated along the Antarctic Peninsula and West Antarctica. The only East Antarctic coastal sector experiencing simultaneous calving front retreat of several glaciers was Wilkes Land in 2009-2018. The largest proportion of calving originated from Ross West and Ronne Ice Shelf being responsible for 75 % of the West Antarctic loss during 1997 and 2008 but was found to be in the range of their natural calving cycle. Decreasing sea ice days, strengthening westerlies, intense snowmelt and increasing sea surface temperatures were identified as driving forces for glacier and ice shelf front retreat along the Antarctic Peninsula, West Antarctica and Wilkes Land. In contrast, relative increases in mean air temperatures could not be linked to calving front retreat. Further studies should assess whether record high air temperatures can also trigger glacier/ice shelf retreat as it has been observed for Greenland. Snowmelt was found to be a strong driver of calving front retreat at the Antarctic Peninsula (up to 5 mm w. eq. per day) but more accurate data on surface melt and surface hydrology is needed to assess the influence of melt in more detail. Increased sea surface temperatures with up to 0.62°C were observed along the Bellingshausen and Amundsen Sea weakening the glacier margins. Between 1997 and 2018, sea ice days decreased most along the Western Antarctic Peninsula with up to -25 days, the Bellingshausen Sea (-10 days) and Amundsen Sea (-5 days). Strengthening westerlies affected ice shelves along the Western Antarctic Peninsula (up to +0.54 m/s) and West Antarctica (+0.28-0.41 m/s) but also East Antarctica at Wilkes (+ 0.44 m/s) and Queen Mary Land (up to 1.23 m/s) by causing upwelling of warm CWD and resulting basal melt. The magnitude of required forcing to immediately trigger calving front retreat was difficult to assess as the regional setting (e.g. bed topography, glacier morphology) as well as the combination and duration of driving forces are likewise important for assessing glacier and ice shelf front retreat. All identified drivers are closely connected to positive phases of SAM which occurred over the last two decades with local maxima forcing stronger retreat. Rising CO_2-emissions and ozone depletion will further enhance positive phases of SAM putting additional pressure on glaciers and ice shelves. To better asses the vulnerability of glaciers and ice shelves in the future, it is essential to better understand melt, ponding and runoff processes on the ice shelf surface impacting calving front retreat to an unknown extent. Equally important is the understanding of changing wind conditions and their impact on upwelling CWD and basal melt. Another interesting issue related to glacier and ice shelf changes across Antarctica pertains to their specific time scales and response times. A shortcoming of our analysis is the restriction to three snapshots of coastline data that has delimited the design of this study. Although our study has revealed that the Antarctic cryosphere is subject to tremendous changes in recent decades, it is conceivable that our results are at least partly biases by strong inter-annual variability of all considered climate and cryospheric variables. In addition, natural cycles and the effects of man-made global warming may prevail on longer time scales than the ones addressed in thus study – the ones that are also characterized by a reasonable data coverage.

Acknowledgements

We thank the Copernicus Climate Data Store for providing the ERA5 climate data and the Ocean and Sea Ice Satellite Application Facility (OSI SAF) for providing the sea ice concentration datasets. In addition, we thank the European Union Copernicus program providing Sentinel-1 data accessible via NASA Alaska Satellite Facility (ASF) and G. J. Marshall for granting open access to the Southern Annular Mode (SAM) Index.

References

Baumhoer, Dietz, A., Dech, S. and Kuenzer, C.: Remote Sensing of Antarctic Glacier and Ice-Shelf Front Dynamics—A Review, Remote Sens., 10(9), 1445, doi:10.3390/rs10091445, 2018.

Baumhoer, C. A., Dietz, A. J., Kneisel, C. and Kuenzer, C.: Automated Extraction of Antarctic Glacier and Ice Shelf Fronts from Sentinel-1 Imagery Using Deep Learning, Remote Sens., 11(21), 2529, doi:10.3390/rs11212529, 2019.

Belmonte Rivas, M. and Stoffelen, A.: Characterizing ERA-Interim and ERA5 surface wind biases using ASCAT, Ocean Sci., 15(3), 831–852, doi:10.5194/os-15-831-2019, 2019.

Brandt-Kreiner, M., Lavelle, J., Tonboe, R., Howe, E., Lavergne, T., Killie, M. A., Sorensen, A., Eastwood, S. and Neuville, A.: Global Sea Ice ConcentrationClimate Data RecordValidation Report. OSI-450 and OSI-430-b. [online] Available from: http://osisaf.met.no/docs/osisaf_cdop3_ss2_valrep_sea-ice-conc-climate-data-record_v1p1.pdf, 2019.

Braun, M., Humbert, A. and Moll, A.: Changes of Wilkins Ice Shelf over the past 15 years and inferences on its stability, The Cryosphere, 3(1), 41–56, doi:10.5194/tc-3-41-2009, 2009.

C3S: Copernicus Climate Change Service. ERA5: Fifth generation of ECMWF atmospheric reanalyses of the global climate, Copernic. Clim. Change Serv. Clim. Data Store CDS [online] Available from: https://cds.climate.copernicus.eu/cdsapp#!/home (Accessed 5 February 2020), 2017.

https://doi.org/10.5194/tc-2020-224
Preprint. Discussion started: 21 September 2020

Cape, M. R., Vernet, M., Skvarca, P., Marinsek, S., Scambos, T. A. and Domack, E.: Foehn winds link climate-driven warming to ice shelf evolution in Antarctica: Foehn winds link climate driven warming, J. Geophys. Res. Atmospheres, 120(21), 11,037-11,057, doi:10.1002/2015JD023465, 2015.

Catania, G. A., Stearns, L. A., Sutherland, D. A., Fried, M. J., Bartholomaus, T. C., Morlighem, M., Shroyer, E. and Nash, J.: Geometric Controls on Tidewater Glacier Retreat in Central Western Greenland, J. Geophys. Res. Earth Surf., 123(8), 2024–2038, doi:10.1029/2017JF004499, 2018.

Chuter, S. J., Martín-Español, A., Wouters, B. and Bamber, J. L.: Mass balance reassessment of glaciers draining into the Abbot and Getz Ice Shelves of West Antarctica: Getz and Abbot Mass Balance Reassessment, Geophys. Res. Lett., 44(14), 7328–7337, doi:10.1002/2017GL073087, 2017.

Cook, A. J. and Vaughan, D. G.: Overview of areal changes of the ice shelves on the Antarctic Peninsula over the past 50 years, The Cryosphere, 4(1), 77–98, doi:10.5194/tc-4-77-2010, 2010.

Cook, A. J., Holland, P. R., Meredith, M. P., Murray, T., Luckman, A. and Vaughan, D. G.: Ocean forcing of glacier retreat in the western Antarctic Peninsula, Science, 353(6296), 283–286, 2016.

Cowton, T. R., Sole, A. J., Nienow, P. W., Slater, D. A. and Christoffersen, P.: Linear response of east Greenland's tidewater glaciers to ocean/atmosphere warming, Proc. Natl. Acad. Sci., 115(31), 7907–7912, doi:10.1073/pnas.1801769115, 2018.

Darelius, E., Fer, I. and Nicholls, K. W.: Observed vulnerability of Filchner-Ronne Ice Shelf to wind-driven inflow of warm deep water, Nat. Commun., 7(1), 12300, doi:10.1038/ncomms12300, 2016.

De Rydt, J., Gudmundsson, G. H., Rott, H. and Bamber, J. L.: Modeling the instantaneous response of glaciers after the collapse of the Larsen B Ice Shelf, Geophys. Res. Lett., 42(13), 5355–5363, doi:10.1002/2015GL064355}, 2015.

De Rydt, J., Gudmundsson, G. H., Nagler, T. and Wuite, J.: Calving cycle of the Brunt Ice Shelf, Antarctica, driven by changes in ice shelf geometry, The Cryosphere, 13(10), 2771–2787, doi:10.5194/tc-13-2771-2019, 2019.

Depoorter, M. A., Bamber, J. L., Griggs, J. A., Lenaerts, J. T. M., Ligtenberg, S. R. M., Van den Broeke, M. R. and Moholdt, G.: Calving fluxes and basal melt rates of Antarctic ice shelves, Nature, 502(7469), 89–89, doi:10.1038/nature12567, 2013.

Dirscherl, M., Dietz, A. J., Kneisel, C. and Kuenzer, C.: Automated Mapping of Antarctic Supraglacial Lakes Using a Machine Learning Approach, Remote Sens., 12(7), 1203, doi:10.3390/rs12071203, 2020.

Domack, E., Duran, D., Leventer, A., Ishman, S., Doane, S., McCallum, S., Amblas, D., Ring, J., Gilbert, R. and Prentice, M.: Stability of the Larsen B ice shelf on the Antarctic Peninsula during the Holocene epoch, Nature, 436(7051), 681–685, doi:10.1038/nature03908, 2005.

Dutrieux, P., De Rydt, J., Jenkins, A., Holland, P. R., Ha, H. K., Lee, S. H., Steig, E. J., Ding, Q., Abrahamsen, E. P. and Schroder, M.: Strong Sensitivity of Pine Island Ice-Shelf Melting to Climatic Variability, Science, 343(6167), 174–178, doi:10.1126/science.1244341, 2014.

Embury, O.: Product Quality Assessment Report. Sea Surface Temperature., [online] Available from: http://datastore.copernicus-climate.eu/c3s/published-forms/c3sprod/satellite-sea-surface-temperature/documentation/v2.0/D2.SST.2-v2.1_PQAR_of_v2SST_products_v3.1_APPROVED_Ver1.pdf (Accessed 28 September 2019), 2019.

Ferrigno, Foley, K. M., Swithinbank, C., Williams Jr, R. S. and Dailide, L.: Coastal-Change And Glaciological Map Of The Ronne Ice Shelf Area,Antarctica: 1974–2002, USGS Coast. Change Maps, I-2600-D, 1–11, 2005.

Ferrigno, Foley, K. M., Swithinbank, C. and Williams Jr, R. S.: Coastal-Change and Glaciological Mapof the Northern Ross Ice Shelf Area,Antarctica: 1962–2004, USGS Coast. Change Maps, 1–11, 2007.

Fountain, A. G., Glenn, B. and Scambos, T. A.: The changing extent of the glaciers along the western Ross Sea, Antarctica, Geology, 45(10), 927–930, 2017.

Fretwell, P., Pritchard, H. D., Vaughan, D. G., Bamber, J. L., Barrand, N. E., Bell, R., Bianchi, C., Bingham, R. G., Blankenship, D. D., Casassa, G. and others: Bedmap2: improved ice bed, surface and thickness datasets for Antarctica, The Cryosphere, 7(1), 2013.

Fricker, H. A., Young, N. W., Allison, I. and Coleman, R.: Iceberg calving from the Amery Ice Shelf, East Antarctica, Ann. Glaciol., 34, 241–246–241–246, doi:10.3189/172756402781817581, 2002.

Friedl, P., Seehaus, T. C., Wendt, A., Braun, M. H. and Höppner, K.: Recent dynamic changes on Fleming Glacier after the disintegration of Wordie Ice Shelf, Antarctic Peninsula, The Cryosphere, 12(4), 1347–1365, doi:10.5194/tc-12-1347-2018, 2018.

Fürst, J. J., Durand, G., Gillet-Chaulet, F., Tavard, L., Rankl, M., Braun, M. and Gagliardini, O.: The safety band of Antarctic ice shelves, Nat. Clim. Change, 6(5), 479–482, 2016.

Gagliardini, O., Durand, G., Zwinger, T., Hindmarsh, R. C. A. and Le Meur, E.: Coupling of ice-shelf melting and buttressing is a key process in ice-sheets dynamics, Geophys. Res. Lett., 37(14), doi:10.1029/2010gl043334, 2010.

Gardner, A. S., Moholdt, G., Scambos, T. A., Fahnstock, M., Ligtenberg, S., van den Broeke, M. and Nilsson, J.: Increased West Antarctic and unchanged East Antarctic ice discharge over the last 7 years, The Cryosphere, 12(2), 521–547, doi:10.5194/tc-12-521-2018, 2018.

Gossart, A., Helsen, S., Lenaerts, J. T. M., Broucke, S. V., van Lipzig, N. P. M. and Souverijns, N.: An Evaluation of Surface Climatology in State-of-the-Art Reanalyses over the Antarctic Ice Sheet, J. Clim., 32(20), 6899–6915, doi:10.1175/JCLI-D-19-0030.1, 2019.

Hazel, J. E. and Stewart, A. L.: Are the Near-Antarctic Easterly Winds Weakening in Response to Enhancement of the Southern Annular Mode?, J. Clim., 32(6), 1895–1918, doi:10.1175/JCLI-D-18-0402.1, 2019.

Hogg, A. E. and Gudmundsson, G. H.: Impacts of the Larsen-C Ice Shelf calving event, Nat. Clim. Change, 7(8), 540–542, doi:10.1038/nclimate3359, 2017.

Holt, T. O., Glasser, N. F., Quincey, D. J. and Siegfried, M. R.: Speedup and fracturing of George VI Ice Shelf, Antarctic Peninsula, The Cryosphere, 7(3), 373–417, 2013.

Howat, I. M., Joughin, I., Fahnestock, M., Smith, B. E. and Scambos, T. A.: Synchronous retreat and acceleration of southeast Greenland outlet glaciers 2000–06: ice dynamics and coupling to climate, J. Glaciol., 54(187), 646–660, doi:10.3189/002214308786570908, 2008.

Hughes, T.: The weak underbelly of the West Antarctic ice sheet, J. Glaciol., 27(97), 518–525, 1981.

https://doi.org/10.5194/tc-2020-224
Preprint. Discussion started: 21 September 2020

Humbert, A., Gross, D., Müller, R., Braun, M., van de Wal, R. S. W., van den Broeke, M. R., Vaughan, D. G. and van de Berg, W. J.: Deformation and failure of the ice bridge on the Wilkins Ice Shelf, Antarctica, Ann. Glaciol., 51(55), 49–55–49–55, doi:10.3189/172756410791392709, 2010.

IMBIE: Mass balance of the Antarctic Ice Sheet from 1992 to 2017, Nature, 558(7709), 219–222, doi:10.1038/s41586-018-0179-y, 2018.

Jenkins, A., Shoosmith, D., Dutrieux, P., Jacobs, S., Kim, T. W., Lee, S. H., Ha, H. K. and Stammerjohn, S.: West Antarctic Ice Sheet retreat in the Amundsen Sea driven by decadal oceanic variability, Nat. Geosci., 11(10), 733–738, doi:10.1038/s41561-018-0207-4, 2018.

Jezek, K. C.: RADARSAT-1 Antarctic Mapping Project: change-detection and surface velocity campaign, Ann. Glaciol., 34(1), 263–268, 2002.

Joughin, I. and Alley, R. B.: Stability of the West Antarctic ice sheet in a warming world, Nat. Geosci., 4(8), 506–513, 2011.

Kim, K. T., Jezek, K. C. and Sohn, H. G.: Ice shelf advance and retreat rates along the coast of Queen Maud Land, Antarctica, J. Geophys. Res.-OCEANS, 106(C4), 7097–7106, doi:10.1029/2000JC000317}, 2001.

Konrad, H., Shepherd, A., Gilbert, L., Hogg, A. E., McMillan, M., Muir, A. and Slater, T.: Net retreat of Antarctic glacier grounding lines, Nat. Geosci., 11(4), 258–258, 2018.

Kwok, R. and Comiso, J. C.: Spatial patterns of variability in Antarctic surface temperature: Connections to the Southern Hemisphere Annular Mode and the Southern Oscillation: Antarctic Surface Temperature, Geophys. Res. Lett., 29(14), 50-1-50–4, doi:10.1029/2002GL015415, 2002.

Larour, E.: Modelling of rift propagation on Ronne Ice Shelf, Antarctica, and sensitivity to climate change, Geophys. Res. Lett., 31(16), L16404, doi:10.1029/2004GL020077, 2004.

Lavergne, T., Sørensen, A. M., Kern, S., Tonboe, R., Notz, D., Aaboe, S., Bell, L., Dybkjær, G., Eastwood, S., Gabarro, C., Heygster, G., Killie, M. A., Brandt Kreiner, M., Lavelle, J., Saldo, R., Sandven, S. and Pedersen, L. T.: Version 2 of the EUMETSAT OSI SAF and ESA CCI sea-ice concentration climate data records, The Cryosphere, 13(1), 49–78, doi:10.5194/tc-13-49-2019, 2019.

Leeson, A. A., Van Wessem, J. M., Ligtenberg, S. R. M., Shepherd, A., Van Den Broeke, M. R., Killick, R., Skvarca, P., Marinsek, S. and Colwell, S.: Regional climate of the Larsen B embayment 1980–2014, J. Glaciol., 63(240), 683–690, doi:10.1017/jog.2017.39, 2017.

Leeson, A. A., Forster, E., Rice, A., Gourmelen, N. and Wessem, J. M.: Evolution of Supraglacial Lakes on the Larsen B Ice Shelf in the Decades Before it Collapsed, Geophys. Res. Lett., 47(4), doi:10.1029/2019GL085591, 2020.

Liu, H. and Jezek, K. C.: A complete high-resolution coastline of Antarctica extracted from orthorectified Radarsat SAR imagery, Photogramm. Eng. Remote Sens., 70(5), 605–616, doi:10.14358/pers.70.5.605, 2004.

Lovell, A. M., Stokes, C. R. and Jamieson, S. S. R.: Sub-decadal variations in outlet glacier terminus positions in Victoria Land, Oates Land and George V Land, East Antarctica (1972–2013), Antarct. Sci., 29(5), 468–483–468–483, doi:10.1017/S0954102017000074, 2017.

Ludescher, J., Yuan, N. and Bunde, A.: Detecting the statistical significance of the trends in the Antarctic sea ice extent: an indication for a turning point, Clim. Dyn., 53(1–2), 237–244, doi:10.1007/s00382-018-4579-3, 2019.

https://doi.org/10.5194/tc-2020-224
Preprint. Discussion started: 21 September 2020

Marshall, G. J.: Trends in the Southern Annular Mode from Observations and Reanalyses, J. Clim., 16, 10, 2003.

Marshall, G. J.: Half-century seasonal relationships between the Southern Annular mode and Antarctic temperatures, Int. J. Climatol., 27(3), 373–383, doi:10.1002/joc.1407, 2007.

Mercer, J. H.: West Antarctic ice sheet and CO2 greenhouse effect: a threat of disaster, Nature, 271(5643), 321–325, 1978.

Miles, B. W. J., Stokes, C. R. and Jamieson, S. S. R.: Pan–ice-sheet glacier terminus change in East Antarctica reveals sensitivity of Wilkes Land to sea-ice changes, Sci. Adv., 2(5), e1501350, doi:10.1126/sciadv.1501350, 2016.

Miles, B. W. J., Stokes, C. R., Jenkins, A., Jordan, J. R., Jamieson, S. S. R. and Gudmundsson, G. H.: Intermittent structural weakening and acceleration of the Thwaites Glacier Tongue between 2000 and 2018, J. Glaciol., 1–11, doi:10.1017/jog.2020.20, 2020.

Milillo, P., Rignot, E., Rizzoli, P., Scheuchl, B., Mouginot, J., Bueso-Bello, J. and Prats-Iraola, P.: Heterogeneous retreat and ice melt of Thwaites Glacier, West Antarctica, Sci. Adv., 5(1), eaau3433, doi:10.1126/sciadv.aau3433, 2019.

Mosbeux, C., Wagner, T. J. W., Becker, M. K. and Fricker, H. A.: Viscous and elastic buoyancy stresses as drivers of ice-shelf calving, J. Glaciol., 1–15, doi:10.1017/jog.2020.35, 2020.

Mouginot, J.: MEaSURES Antarctic Boundaries for IPY 2007-2009 from Satellite Radar, Version 2, , doi:10.5067/AXE4121732AD, 2017.

Mouginot, J., Rignot, E. and Scheuchl, B.: Continent-Wide, Interferometric SAR Phase, Mapping of Antarctic Ice Velocity, Geophys. Res. Lett., 46(16), 9710–9718, doi:10.1029/2019GL083826, 2019.

Nakamura, K., Doi, K. and Shibuya, K.: Why is Shirase Glacier turning its flow direction eastward?, Polar Sci., 1(2), 63–71, doi:10.1016/j.polar.2007.09.003, 2007.

Nicholls, K. W., Østerhus, S., Makinson, K., Gammelsrød, T. and Fahrbach, E.: Ice-ocean processes over the continental shelf of the southern Weddell Sea, Antarctica: A review, Rev. Geophys., 47(3), 2009.

NSIDC: Natl. Snow Ice Data Cent. RAMP AMM-1 SAR Image Mosaic Antarct. Version 2 [online] Available from: https://nsidc.org/data/NSIDC-0103/versions/2 (Accessed 3 January 2020), 1997.

NSIDC: Natl. Snow Ice Data Cent. MODIS Mosaic Antarct. 2008-2009 MOA2009 Image Map Version 1 [online] Available from: https://nsidc.org/data/NSIDC-0593/versions/1 (Accessed 3 May 2020), 2009.

Osisaf: Ocean and Sea Ice Satellite Application Facility. High Latitude Products. Sea Ice Concentration., [online] Available from: http://osisaf.met.no/p/ice/ (Accessed 3 February 2020), 2020.

Paeth, H. and Pollinger, F.: Enhanced evidence in climate models for changes in extratropical atmospheric circulation, Tellus Dyn. Meteorol. Oceanogr., 62(5), 647–660, doi:10.1111/j.1600-0870.2010.00455.x, 2010.

Paolo, F. S., Fricker, H. A. and Padman, L.: Volume loss from Antarctic ice shelves is accelerating, Science, 348(6232), 327–331, 2015.

Parkinson, C. L.: A 40-y record reveals gradual Antarctic sea ice increases followed by decreases at rates far exceeding the rates seen in the Arctic, Proc. Natl. Acad. Sci., 116(29), 14414–14423, doi:10.1073/pnas.1906556116, 2019.

Rack, W. and Rott, H.: Pattern of retreat and disintegration of the Larsen B ice shelf, Antarctic Peninsula, Ann. Glaciol., 39(1), 505–510, 2004.

Rankl, M., Fürst, J. J., Humbert, A. and Braun, M. H.: Dynamic changes on the Wilkins Ice Shelf during the 2006--2009 retreat derived from satellite observations, The Cryosphere, 11(3), 1199–1211, doi:10.5194/tc-11-1199-2017, 2017.

Rignot, E., Mouginot, J. and Scheuchl, B.: Ice Flow of the Antarctic Ice Sheet, Science, 333(6048), 1427–1430, doi:10.1126/science.1208336, 2011.

Rignot, E., Jacobs, S., Mouginot, J. and Scheuchl, B.: Ice-Shelf Melting Around Antarctica, Science, 341(6143), 266–270, doi:10.1126/science.1235798, 2013.

Rignot, E., Mouginot, J., Scheuchl, B., van den Broeke, M., van Wessem, M. J. and Morlighem, M.: Four decades of Antarctic Ice Sheet mass balance from 1979–2017, Proc. Natl. Acad. Sci., 116(4), 1095–1103, doi:10.1073/pnas.1812883116, 2019.

Rott, H., Müller, F., Nagler, T. and Floricioiu, D.: The imbalance of glaciers after disintegration of Larsen-B ice shelf, Antarctic Peninsula, The Cryosphere, 5(1), 125–125, 2011.

Royston, S. and Gudmundsson, G. H.: Changes in ice-shelf buttressing following the collapse of Larsen A Ice Shelf, Antarctica, and the resulting impact on tributaries, J. Glaciol., 62(235), 905–911, 2016.

Scambos, T. A., Haran, T. M., Fahnestock, M. A., Painter, T. H. and Bohlander, J.: MODIS-based Mosaic of Antarctica (MOA) data sets: Continent-wide surface morphology and snow grain size, Remote Sens. Environ., 111(2), 242–257, doi:10.1016/j.rse.2006.12.020, 2007.

Scambos, T. A., Fricker, H. A., Liu, C.-C., Bohlander, J., Fastook, J., Sargent, A., Massom, R. and Wu, A.-M.: Ice shelf disintegration by plate bending and hydro-fracture: Satellite observations and model results of the 2008 Wilkins ice shelf break-ups, Earth Planet. Sci. Lett., 280(1), 51–60, doi:10.1016/j.epsl.2008.12.027, 2009.

Scheuchl, B., Mouginot, J., Rignot, E., Morlighem, M. and Khazendar, A.: Grounding line retreat of Pope, Smith, and Kohler Glaciers, West Antarctica, measured with Sentinel-1a radar interferometry data, Geophys. Res. Lett., 43(16), 8572–8579, doi:10.1002/2016GL069287, 2016.

Seroussi, H., Nakayama, Y., Larour, E., Menemenlis, D., Morlighem, M., Rignot, E. and Khazendar, A.: Continued retreat of Thwaites Glacier, West Antarctica, controlled by bed topography and ocean circulation, Geophys. Res. Lett., 44(12), 6191–6199, doi:10.1002/2017GL072910, 2017.

Spence, P., Griffies, S. M., England, M. H., Hogg, A. McC., Saenko, O. A. and Jourdain, N. C.: Rapid subsurface warming and circulation changes of Antarctic coastal waters by poleward shifting winds: Antarctic subsurface ocean warming, Geophys. Res. Lett., 41(13), 4601–4610, doi:10.1002/2014GL060613, 2014.

Stewart, A. L., Klocker, A. and Menemenlis, D.: Circum-Antarctic Shoreward Heat Transport Derived From an Eddy- and Tide-Resolving Simulation, Geophys. Res. Lett., 45(2), 834–845, doi:10.1002/2017GL075677, 2018.

Tamura, T., Williams, G. D., Fraser, A. D. and Ohshima, K. I.: Potential regime shift in decreased sea ice production after the Mertz Glacier calving, Nat. Commun., 3(1), 826, doi:10.1038/ncomms1820, 2012.

Tedesco, M. and Monaghan, A. J.: An updated Antarctic melt record through 2009 and its linkages to high-latitude and tropical climate variability, Geophys. Res. Lett., 36(18), L18502, doi:10.1029/2009GL039186, 2009.

https://doi.org/10.5194/tc-2020-224
Preprint. Discussion started: 21 September 2020

Tetzner, D., Thomas, E. and Allen, C.: A Validation of ERA5 Reanalysis Data in the Southern Antarctic Peninsula—Ellsworth Land Region, and Its Implications for Ice Core Studies, Geosciences, 9(7), 289, doi:10.3390/geosciences9070289, 2019.

Thoma, M., Jenkins, A., Holland, D. and Jacobs, S.: Modelling Circumpolar Deep Water intrusions on the Amundsen Sea continental shelf, Antarctica, Geophys. Res. Lett., 35(18), L18602, doi:10.1029/2008GL034939, 2008.

Trusel, L. D., Frey, K. E., Das, S. B., Munneke, P. K. and van den Broeke, M. R.: Satellite-based estimates of Antarctic surface meltwater fluxes: Satellite-Based Antarctic Melt Fluxes, Geophys. Res. Lett., 40(23), 6148–6153, doi:10.1002/2013GL058138, 2013.

Vaughan, D. G. and Doake, C. S. M.: Recent atmospheric warming and retreat of ice shelves on the Antarctic Peninsula, Nature, 379(6563), 328–328, 1996.

Verdy, A., Marshall, J. and Czaja, A.: Sea surface temperature variability along the path of the Antarctic Circumpolar Current., J. Phys. Oceanogr., 36(7), 1317–1331, 2006.

Walker, C. C. and Gardner, A. S.: Rapid drawdown of Antarctica's Wordie Ice Shelf glaciers in response to ENSO/Southern Annular Mode-driven warming in the Southern Ocean, Earth Planet. Sci. Lett., 476, 100–110, doi:10.1016/j.epsl.2017.08.005, 2017.

Wang, G., Cai, W. and Purich, A.: Trends in Southern Hemisphere wind-driven circulation in CMIP5 models over the 21st century: Ozone recovery versus greenhouse forcing, J. Geophys. Res. Oceans, 119(5), 2974–2986, doi:10.1002/2013JC009589, 2014.

Wouters, B., Martin-Espanol, A., Helm, V., Flament, T., van Wessem, J. M., Ligtenberg, S. R. M., van den Broeke, M. R. and Bamber, J. L.: Dynamic thinning of glaciers on the Southern Antarctic Peninsula, Science, 348(6237), 899–903, doi:10.1126/science.aaa5727, 2015.

Yu, H., Rignot, E., Morlighem, M. and Seroussi, H.: Iceberg calving of Thwaites Glacier, West Antarctica: full-Stokes modeling combined with linear elastic fracture mechanics, CRYOSPHERE, 11(3), 1283–1296, doi:10.5194/tc-11-1283-2017}, 2017.